

NASA CR-135150

# DEVELOPMENT OF OXIDE DISPERSION STRENGTHENED TURBINE BLADE ALLOY BY MECHANICAL ALLOYING

by

H.F. Merrick, L.R. Curwick and Y.G. Kim

(NASA-CR-135150) DEVELOPMENT OF OXIDE  
DISPERSION STRENGTHENED TURBINE BLADE ALLOY  
BY MECHANICAL ALLOYING (International Nickel  
Co., Inc.) 69 F EC A04/EF A01 CSCI 11F

N77-22213

Unclas  
63/26 25110

Prepared for

**NATIONAL AERONAUTICS  
AND SPACE ADMINISTRATION**

**Lewis Research Center**

Contract NAS 3-19694

T.K. Glasgow, Project Manager



**Inco**

**THE INTERNATIONAL NICKEL COMPANY, INC.**  
**PAUL D. MERICA RESEARCH LABORATORY**  
**SUFFERN, NEW YORK 10901**

DEVELOPMENT OF AN OXIDE DISPERSION STRENGTHENED  
TURBINE BLADE ALLOY BY MECHANICAL ALLOYING

H.F. Merrick, L.R. Curwick and Y.G. Kim

January 1977

THE INTERNATIONAL NICKEL COMPANY, INC.  
PAUL D. MERICA RESEARCH LABORATORY

Prepared for

NATIONAL AERONAUTICS AND SPACE ADMINISTRATION

NASA-Lewis Research Center  
Contract NAS3-19694  
FINAL REPORT

1. Report No. NASA CR-135150		2. Government Accession No.		3. Recipient's Catalog No.	
4. Title and Subtitle DEVELOPMENT OF AN OXIDE DISPERSION STRENGTHENED TURBINE BLADE ALLOY BY MECHANICAL ALLOYING				5. Report Date JANUARY 1977	
				6. Performing Organization Code	
7. Author(s) H.F. MERRICK, L.R. CURWICK AND Y.G. KIM				8. Performing Organization Report No.	
9. Performing Organization Name and Address THE INTERNATIONAL NICKEL COMPANY, INC. SUFFERN, NY 10901				10. Work Unit No.	
				11. Contract or Grant No. NAS3-19694	
12. Sponsoring Agency Name and Address NATIONAL AERONAUTICS AND SPACE ADMINISTRATION, WASHINGTON, DC 20546				13. Type of Report and Period Covered CONTRACTOR REPORT	
				14. Sponsoring Agency Code	
15. Supplementary Notes PROJECT MANAGER, THOMAS K. GLASGOW, MATERIALS AND STRESSES DIVISION, NASA-LEWIS RESEARCH CENTER, CLEVELAND, OH					
16. Abstract Three nickel-base alloys containing up to 18 wt. % of refractory metal were examined initially for oxide dispersion strengthening. To provide greater processing freedom, however, a leaner alloy was finally selected. This base alloy, "alloy D", contained 0.05C/15Cr/2Mo/4W/2Ta/4.5Al/2.5Ti/0.15Zr/0.01B/Bal. Ni. Following alloy selection, the effect of extrusion, heat treatment and oxide volume fraction and size on microstructure and properties were examined. The optimum structure was achieved in zone annealed alloy D which contained 2.5 vol. % of 35-nm Y <sub>2</sub> O <sub>3</sub> and which was extruded 16:1 at 1038°C (1900°F). The optimum 100 hour rupture strength was 165 MPa (24 ksi) at 1093°C (2000°F) and 551 MPa (80 ksi) at 760°C (1400°F). Rupture elongation was typically 2.5% at both temperatures. Alloy D has good oxidation resistance and excellent sulfidation resistance similar to alloy 713C and IN-792 respectively.					
17. Key Words (Suggested by Author(s)) OXIDE DISPERSION STRENGTHENING NICKEL-BASE SUPERALLOYS MECHANICAL ALLOYING YTTRIUM OXIDE GAMMA PRIME				18. Distribution Statement  UNCLASSIFIED - UNLIMITED	
19. Security Classif. (of this report) UNCLASSIFIED		20. Security Classif. (of this page) UNCLASSIFIED		21. No. of Pages	
				22. Price*	

\* For sale by the National Technical Information Service, Springfield, Virginia 22151

## TABLE OF CONTENTS

	<u>Page</u>
I. SUMMARY . . . . .	1
II. INTRODUCTION . . . . .	2
III. EXPERIMENTAL PROCEDURE . . . . .	3
A. Attritor Processing . . . . .	3
B. Extrusion . . . . .	3
C. Heat Treatment . . . . .	3
D. Mechanical Tests . . . . .	4
E. Oxidation Tests . . . . .	4
F. Sulfidation Tests . . . . .	4
G. Phase Extraction and Analysis . . . . .	5
IV. EXPERIMENTAL RESULTS AND DISCUSSION . . . . .	5
A. Preliminary Alloy Study . . . . .	5
Attritor Processing . . . . .	6
Extrusion . . . . .	6
Recrystallization Response . . . . .	7
Stress Rupture Properties . . . . .	7
B. Alloy D Powder Processing and Consolidation . . . . .	8
C. Recrystallization Response of Alloy D . . . . .	9
D. 1093°C (2000°F) Stress Rupture Properties of Alloy D . . . . .	10
Effect of Grain Structure on the 1093°C (2000°F) Rupture Life . . . . .	10
Effect of Dispersoid Variables on the 1093°C (2000°F) Rupture Life . . . . .	11
E. 760°C (1400°F) Stress Rupture Properties . . . . .	11
F. Tensile Properties of Alloy D . . . . .	14
G. Oxidation and Sulfidation Resistances of Alloy D . . . . .	14
H. Characteristics of $\gamma'$ and Oxide Dispersion of Alloy D . . . . .	14
$\gamma'$ Phase . . . . .	14
Oxide Dispersion . . . . .	15
V. CONCLUSION . . . . .	15
VI. REFERENCES . . . . .	17

TABLES I-XIV

FIGURES 1-24

## I. SUMMARY

Oxide dispersion strengthened nickel-base alloys are currently under development for application to advanced gas turbine engines. The objective of this program was to develop an oxide dispersion strengthened nickel-base superalloy for turbine blade applications using the mechanical alloying process. The alloy was to possess a 100 hour rupture life capability of 172 MPa (25 ksi) at 1093°C (2000°F) and 483 MPa (70 ksi) at 760°C (1400°F), adequate ductility and corrosion resistance and be capable of being coated. To achieve the objectives, several oxide dispersion strengthened nickel-base superalloys were prepared. After initial trials, an alloy was selected which responded favorably to mechanical alloying, yielding excellent microstructures over a range of processing variables. The base alloy contained .05C/15Cr/2Mo/4W/4.5Al/2.5Ti/2Ta/.15Zr/.01B/Bal. Ni, and was designated alloy D.

The effects of varying dispersoid parameters in alloy D on the 1093°C (2000°F) rupture strength showed that the powder blend containing 2.5 vol. % with 35 nm diameter  $Y_2O_3$  particles exhibited the highest strength. The 100 hour rupture strength capability of the alloy at 1093°C (2000°F) is 165 MPa (24 ksi). This is the highest strength ever achieved in an oxide dispersion strengthened alloy designed for turbine blade applications. The projected 1000 hour rupture life capability of the alloy at 1149°C (2100°F) is about 103 MPa (15 ksi). In comparison with the 1000 hour rupture life of other alloys, alloy D shows a strength superiority over DS Mar M-200 + Hf above about 871°C (1600°F) and the  $\gamma/\gamma'-\delta$  DS eutectic alloy (Ni-20Nb-6Cr-2.5Al) above about 960°C (1760°F).

The 100 hour rupture strength of the alloy D at 760°C (1400°F), and 551 MPa (80 ksi), exceeded the 100 hour life target strength of 483 MPa (70 ksi). A heat treatment imposing an intermediate 954°C (1950°F) annealing prior to final aging gave the best combination of high strength and ductility. It provided an elongation of about 2.5 percent together with a rupture life at 551 MPa (80 ksi) of 75-170 hours.

Alloy D has good oxidation resistance at 1100°C (2012°F) and is about equal to IN-100 and alloy 713 LC. The sulfidation resistance of alloy D is comparable to the cast nickel-base alloys IN-738 and IN-792.

## II. INTRODUCTION

Improved gas turbine performance and efficiency depends to a large extent on increasing the operating temperature. Increasing the turbine inlet temperature must be tied to corresponding advances in material capability, particularly turbine blade materials. Currently, improved blade material capability is being actively sought on three fronts, i.e. directional solidification (DS) of superalloys and eutectics, refractory wire reinforced superalloy composites, and oxide dispersion strengthened alloys (ODS) (ref. 1). Ceramics ( $\text{SiC}$  and  $\text{Si}_3\text{N}_4$ ) are also under consideration but a major breakthrough in terms of ductility and impact resistance is needed before these materials can be employed as blade materials in aircraft gas turbine engines.

Following the application of directional solidification to conventional superalloys, e.g. Mar-M-200 + Hf, research is now being focused on the development of eutectic systems. Directionally solidified eutectics have a potential advantage of 30-80°C (50-150°F) over the best currently used DS superalloys. Two classes of alloys are under active evaluation, i.e. lamellar  $\gamma/\gamma'-\delta$  alloys, Ni-20Cb-6Cr-2.5Al, and rod reinforced alloys, NiTaC (ref. 2) and  $\gamma/\gamma'-\alpha$  (ref. 3).

In the area of composites, tungsten and tungsten-hafnium-carbon wire reinforced alloys promise use temperatures exceeding those of the eutectic systems. Fiber-matrix interaction and thermal and mechanical fatigue are current problem areas. However, recently significant progress has been made for a W-1%ThO<sub>2</sub>/FeCrAlY system (ref. 1).

The third approach, that of oxide dispersion strengthened systems, has been under active development at the Paul D. Merica Research Laboratory of The International Nickel Company, Inc. (Inco). Alloys for turbine vane applications, e.g. alloy MA 754, are currently being evaluated commercially. ODS turbine blade alloys, in which oxide dispersion strengthening is coupled with  $\gamma'$  strengthening have also been under study. The ability to combine these strengthening mechanisms using the mechanical alloying process was first demonstrated by Benjamin (ref. 4) and Benjamin and Cairns (refs. 5 and 6). More recently alloys containing a higher volume fraction of  $\gamma'$  have been evaluated (refs. 7 and 8). High temperature strength of ODS alloys is principally controlled by the characteristic elongated grain structure. The influence of grain aspect ratio has been discussed by Wilcox and Clauer (ref. 9) and Cairns et al (ref. 7). Intermediate temperature strength is due to the dispersion of  $\gamma'$  precipitates.

The objectives of this research program were to develop a mechanically alloyed nickel-base superalloy that would possess a 100 hour rupture life capability of 172 MPa (25 ksi) at 1093°C (2000°F) and 482 MPa (70 ksi) at 760°C (1400°F) while retaining adequate ductility. In addition the alloy should display adequate corrosion resistance and be capable of being coated.

### III. EXPERIMENTAL PROCEDURE

#### A. Attritor Processing

The following powders were used for mechanical alloying:

- Nickel, Type 123
- Elemental Chromium
- Elemental Molybdenum
- Elemental Tungsten
- Elemental Tantalum
- Titanium, Ni-17Al-28Ti Master Alloy
- Aluminum, Ni-46Al Master Alloy
- Zirconium, Ni-29Zr Master Alloy
- Boron, Ni-18B Master Alloy
- Y<sub>2</sub>O<sub>3</sub> (Calcined Yttrium Oxalate)

Powders containing an intimate dispersion of yttrium oxide were prepared by milling in a high energy, stirred ball mill (ref. 4). Powder homogeneity was checked by optical microscopy.

#### B. Extrusion

After screening to remove the coarse +12 mesh particles, powder batches were cone blended for two hours and packed into 8.8 cm (3.5 in) OD and .63 cm (0.25 in) wall thickness mild steel extrusion cans. Each can was evacuated to about 30µm pressure at 593°C (1100°F) for three hours. They were then cooled and sealed under vacuum. Extrusion was performed at temperatures of 1038°C (1900°F), 1066°C (1950°F) and 1093°C (2000°F), using reductions of 12:1, 16:1, 20:1, and 22:1.

#### C. Heat Treatment

Isothermal gradient annealing was used to determine the recrystallization response of extruded bar. The annealing was performed in a gradient furnace shown in Figure 1. The temperature profile of the furnace is also shown in Figure 1. The gradient annealed bar was polished parallel

to the extrusion direction and etched to examine the recrystallization response. From the gradient annealing study, an optimum temperature for zone annealing was selected. Zone annealing was conducted to produce high grain aspect ratio (GAR) since a high GAR is essential for high temperature strength in ODS alloys (refs. 7,9,10 and 11). Extruded bars were zone annealed in the same gradient furnace by moving the furnace at a speed of 13.5 cm/hr (5.3 in/hr) with the maximum hot zone temperature at 1232°C (2250°F).

#### D. Mechanical Tests

Specimens for stress rupture and tensile tests were prepared from extruded and subsequently zone annealed bar. All tests were performed in air with the tensile axis parallel to the extrusion direction. The test specimens had a 0.32 cm (0.125 in) gage diameter and a gage length of 2.54 cm (1.0 in). The stress rupture and tensile elongations were measured by the increased gage length after fitting back the broken test specimens. All tests conformed to ASTM specifications.

#### E. Oxidation Tests

Cyclic oxidation tests were performed in low velocity (.5 cm/sec) air-5% $H_2O$  at 1100°C (2012°F) for a total period of 504 hours. After each 24 hour interval the specimens were rapidly cooled to room temperature and the weight change recorded. After the final weight change measurement, the samples were descaled by a light abrasion with  $Al_2O_3$  grit blast. Test specimens were 1.9 cm (0.75 in) long and .76 cm (.3 in) diameter.

#### F. Sulfidation Tests

Sulfidation tests were performed at 927°C (1700°F) in a low velocity (.023 Mach) burner rig (ref. 12). This test ran on a one hour cycle, 58 minutes rotating in the flame, two minutes in air blast. The flame conditions were a 30:1 air + 5 ppm seawater (ASTM Spec. D1141-52) to fuel (.3% sulfur JP-5) ratio. The specimens, 3.8 cm (1.5 in) long and 0.3 cm (0.125 in) diameter, were weighed each 24 hours and standard diametric (cross section) metal loss and grain boundary penetration measurements were made at the end of the test. Descaled weight loss was also determined.



#### G. Phase Extraction and Analysis

Samples of the alloys were dissolved in two different extraction media. The  $\gamma'$  precipitate was extracted from samples of heat treated [zone annealed + 1/2 hr/1232°C (2250°F)/AC + 24 hrs/843°C (1550°F)/AC] bar using anodic dissolution in an electrolyte consisting of 1% ammonium sulfate and 1% citric acid in water (ref. 13). Since this solution will also extract carbides, nitrides and oxides, a separate extraction was performed using 10% HCl + 1% tartaric acid in methanol to selectively extract these phases. In this way the weight percent of  $\gamma'$  and carbides + nitrides + oxides could be calculated.

Phase identification was performed using a Siemens x-ray diffractometer fitted with a graphite crystal monochromator and employing copper radiation at 30 kV and 38 mA. The  $2\theta$  scan rate was 2° per minute.

### IV. EXPERIMENTAL RESULTS AND DISCUSSION

#### A. Preliminary Alloy Study

The chemical compositions of three alloys selected for initial evaluation are shown in Table I. In considering the need to assure high inherent oxidation resistance, the aluminum level was set at 4.5%. The levels of chromium, tungsten, titanium and tantalum were chosen to impart adequate sulfidation resistance. The aluminum, titanium and tantalum levels were considered satisfactory for providing adequate  $\gamma'$  forming potential for intermediate temperature strength.

In selecting these alloy compositions due cognizance was also taken of the need for alloy stability, i.e. freedom from the development of deleterious phases, such as sigma phase, upon stressed exposure at intermediate temperatures. Electron vacancy numbers for both residual matrix,  $N_V(\gamma)$ , and  $\gamma'$  precipitate,  $N_V(\gamma')$  were determined for the three alloys using a computer program developed at Inco. The results were as follows:

	$N_V(\gamma)$	$N_V(\gamma')$
Alloy A	2.87	2.20
Alloy B	2.88	2.16
Alloy C	2.92	2.17

The electron vacancy numbers for the residual matrix [ $N_V(\gamma)$ ] are higher than would be judged safe for cast nickel-base superalloys with their attendant compositional segregation effects. The upper limit of  $N_V(\gamma)$  for mechanically alloyed nickel-base superalloys has not yet been defined at present.

Attritor Processing. Two attritor processing runs were made of alloy A and one each of alloys B and C. The screen analyses of the three powder batches are shown in Table II. Similar powder size distributions were obtained for batches N2, N3 and N4. Each batch had a high -325 mesh fraction ranging from about 21 to 23 percent. Powder batch N1 was somewhat coarser and had a lower -325 mesh fraction (7.4 percent).

Metallographic examination of samples of each powder batch were etched two minutes in a 50/50 cyanide-persulfate etchant. This etchant was used to reveal possible inhomogeneities in the product such as chromium fragments and hence provide a gauge as to the degree of processing obtained during attriting. Examples of the powder structure are shown in Figures 2 and 3. For each powder batch there was very little difference between the three alloys in terms of attritor processability. Since a chromium level of 16 percent would be beneficial from the sulfidation standpoint and a tungsten level of 10 percent desirable to provide added solid solution strengthening, it was felt that alloy A was the best candidate for further evaluation.

Additional powder of alloy A was prepared using the same attritor processing conditions as previously. The screen analysis for each powder batch is listed in Table III. Samples from each batch were evaluated metallographically to check powder homogeneity. Excellent powder homogeneity was maintained for each powder batch although, as indicated in Table III, some variation in mesh size distribution occurred. Following screening, the -12 mesh fraction of all listed powder batches were cone blended together. This combined powder blend was designated N23. The average oxygen and nitrogen content of the powder blend was 0.62 and 0.074 percent respectively.

Extrusion. Cone blended powder was sealed in 8.57 cm (3.375 in) diameter cans having a wall thickness of 1.27 cm (0.5 in). Extrusion was performed at temperatures of 1038°C (1900°F), 1066°C (1950°F) and 1093°C (2000°F) using reductions of 12:1, 16:1 and 22:1 respectively. Conical dies having a 90° included angle were employed for extrusion. Lubrication was provided by oil swabbing the heated extrusion chamber, a glass wrap about the extrusion billet and a glass pad on the die face.

Recrystallization Response. Samples of bar from each of the eighteen extrusions were annealed for one-half hour at 1204, 1232, 1260 and 1288°C (2200, 2250, 2300 and 2350°F). Extruded bar which showed the best response to recrystallization using conventional isothermal annealing was subjected to structural evaluation using the traveling gradient annealing furnace (zone annealing). A furnace travel rate of 13.5 to 16.3 cm/hr (5.3 to 6.4 in/hr) was employed for annealing temperatures which ranged between 1230 and 1243°C (2245 and 2270°F). Table IV describes the structures observed and values of the grain aspect ratio (GAR; the ratio of average grain length to grain diameter) in terms of extrusion temperature, ratio and ram speed.

In general terms the results of the extrusion study indicate that the best recrystallization response occurs for the higher extrusion ratios (16:1 and 22:1) at 1038 and 1066°C (1900 and 1950°F). Figures 4a and 4b show the recrystallized microstructures of bar extruded at two different extrusion ratios (12:1, 22:1) at 1066°C (1950°F). Even though ideal elongated grain structures were not obtained (smaller equiaxed grains were always present even for the best grain structures) trend lines indicating the recrystallization response of the alloy with respect to extrusion temperature and ratio can be drawn. The zones of recrystallization response are shown in Figure 5. The observed structural trend suggests that for this alloy lower extrusion temperatures and/or higher ratios may broaden the region for which coarse elongated grain structures are obtained.

Stress Rupture Properties. The 1093°C (2000°F) stress rupture capability of extruded and annealed bar was determined by employing step loading tests. The technique consisted of loading a sample to a stress level of 97 MPa (14 ksi) and maintaining the load for 24 hours. If the sample was unbroken after this period of time, the stress was increased by 14 MPa (2 ksi). Using stress increments of 14 MPa (2 ksi) and time periods of 24 hours the stress rupture capability of extruded bar was determined. Test results are shown in Table V. The best properties were developed for conventionally annealed bar extruded 22:1 at 1038°C (1900°F). However, the rupture strengths were well below the program target level of 172 MPa (25 ksi) for 100 hour life.

In view of the difficulties in producing ideal coarse elongated grain structures in alloy A, it was decided that a modified alloy composition be evaluated. This alloy was designated alloy D (see Table I) and had the following nominal composition: .05C/15Cr/2Mo/4W/4.5Al/2.5Ti/2Ta/.15Zr/.01B/Bal. Ni/1.1Y<sub>2</sub>O<sub>3</sub>. The essential change from alloy A concerned a lowering of the refractory element content; i.e., W from 10 to 4 percent, Mo from 3 to 2 percent, and Ta from 2.5 to 2 percent. The chromium level was also lowered to 15 percent. Electron vacancy numbers for both the residual matrix,  $N_V(\gamma)$ , and  $\gamma'$  precipitate,  $N_V(\gamma')$ , in alloy D were calculated as 2.41 and 2.02 respectively. These are significantly lower than those of alloy A. A sample of alloy A was annealed at 1232°C (2250°F) to develop a coarse grain structure and then exposed at 816°C (1500°F) under an applied stress of 207 MPa (30 ksi) for 2000 hours. After this period the sample was examined metallographically for evidence of  $\sigma$ -phase. Representative replica electron micrographs of the gage section of the test sample are shown in Figure 6. No evidence of an acicular phase indicative of  $\sigma$  precipitation was evident. Since no evidence of  $\sigma$  phase was observed in alloy A, no propensity for the formation of this phase would be expected in alloy D.

#### B. Alloy D Powder Processing and Consolidation

The raw material powders used to prepare alloy D were the same as for alloy A. In order to examine the effects of dispersoid variables (oxide particle size and volume fraction), powder blends containing the following combinations of dispersoid size and volume fraction were processed:

Powder Blend	Y <sub>2</sub> O <sub>3</sub> Volume, %	Avg. Volumetric Diameter	
		Aim	Actual
N40	1.0	50 nm	35 nm
N39	2.5	50 nm	35 nm
N48	2.5	100 nm	45 nm
N56	4.0	100 nm	45 nm

The dispersoid, Y<sub>2</sub>O<sub>3</sub>, was prepared by calcination of yttrium oxalate. For a nominal dispersoid average volumetric diameter of about 50 nm, the oxalate was calcined 16 hours at 704°C (1300°F) (ref. 14). To achieve a coarser particle size (about 100 nm), the oxalate was first calcined at 704°C (1300°F) and then heated 20 hours at 1500°C (2732°F). A subsequent analysis (see section H) showed the actual average volumetric diameter of Y<sub>2</sub>O<sub>3</sub> achieved to be 35 nm for the 704°C (1300°F) calcination and 45 nm for the 1500°C (2732°F) calcination. Higher heat treatment temperatures than 1500°C (2732°F) were not possible because of sintering.

Each batch of attrited powder was examined metallographically after etching for 2 minutes in a 50/50 solution of cyanide persulfate. Powder in each category which was considered to be well processed was screened and the -12 mesh fraction cone blended to provide master stock. Details of the screen analyses of each blend are given in Table VI. Compared with the earlier results for alloy A, the attrited powder of alloy D is much coarser. This is probably related mainly to the lower tungsten level. Differences do exist for each blend and these are related to the level of dispersoid added. The lowest -325 mesh fraction occurs for the lowest level of dispersoid added (N40 at 1.0 volume percent). Increasing the dispersoid level increases the -325 mesh fraction such that for a 4 volume percent loading (N56) it reaches about 12 percent. Attempts were made to adjust attritor processing parameters in order to reduce the -325 mesh fraction of N56 to values closer to N39 and N48 but these were not successful. The higher -325 mesh fraction of N56 did not adversely affect the subsequent secondary recrystallization behavior of the powder.

Powder of each blend was packed into mild steel cans 8.9 cm (3.5 in) diameter 0.64 cm (0.25 in) wall thickness fitted with tapered nose cones. Each can was evacuated to about 30 $\mu$ m pressure and then heated for 3 hours at 816°C (1500°F) prior to sealing. Extrusion employing two temperatures, two ratios and two ram speeds was performed at NASA-Lewis. Extrusion variables used are listed in Table VII.

### C. Recrystallization Response of Alloy D

Samples from the extruded bars listed in Table VII were subjected to gradient annealing to observe the morphology of secondary recrystallized grains and to determine the temperature range to produce elongated grain growth. Bar samples 1.3 cm diameter and 10.2 cm long (.5 in. diameter and 4 in. long) were placed into the gradient furnace with a maximum hot zone temperature of about 1316°C (2400°F). The temperature gradient of the furnace was about 82°C/cm (180°F per in). Total annealing time was 45 minutes, each sample taking about 15 minutes to reach a stable temperature distribution.

Figure 7 shows the grain structures of gradient annealed N39A, B, C and D samples. Approximate temperatures along the bar are indicated. The elongated grains develop from the melting point of the alloy [judged to be approximately 1288°C (2350°F)] to about 1149°C (2100°F) for all extrusion ratios and ram speeds. The recrystallization response does not appear to be too sensitive to the extrusion parameters examined. Figure 8 shows the grain

structures of gradient annealed bars N39E, F, G and H. Again elongated grain structures were produced for these 1093°C (2000°F) extrusions. However, there are differences between the recrystallization response of these bars and those of N39A, B, C and D. The minimum temperature for recrystallization is about 1177°C (2150°F) for bars N39E and N39F and 1204°C (2200°F) for bars N39G and N39H. These temperatures are somewhat higher than those observed for N39A, B, C and D.

Limited gradient annealing studies were performed on extruded bar samples of N40, N48 and N56. Metallographic examination of the gradient annealed bars showed that coarse elongated grain structures were produced. Examples of the structures of N40 and N48 extruded at 1038°C (1900°F) are shown in Figure 9. A poor recrystallization response (very low GAR) was obtained for bar of N56 extruded at a temperature of 1038°C (1900°F) and a ram speed of 20.3 cm/sec (8 in/sec). The poor structural response was attributed to contamination of the powder due to improper sealing of the extrusion can. A subsequent extrusion of clean powder, however, gave essentially the same results.

To produce by recrystallization material having a continuous elongated grain structure (GAR >10:1) for mechanical testing, extruded bar of all conditions was subjected to traveling gradient anneal (zone annealing). An annealing temperature of 1232°C (2250°F) was employed with a furnace travel rate of 13.5 cm/hr (5.3 in/hr). 1232°C (2250°F) appeared to be the optimum temperature from the gradient anneal studies. A typical microstructure of the zone annealed N39B bar of alloy D is shown in Figure 10.

#### D. 1093°C (2000°F) Stress Rupture Properties of Alloy D

Stress rupture data for extruded and annealed bar of alloys N39, N40, N48 and N56 are listed in Table VIII. For each of these alloys the properties of bar extruded at 1038°C (1900°F) are better than those of bar extruded at 1093°C (2000°F). The highest rupture strength was developed for alloy N39B extruded 16:1 at 1038°C (1900°F). The 100 hour rupture strength capability of alloy D (N39B) at 1093°C (2000°F) is 165 MPa (24 ksi) and the projected 1000 hour strength is 158 MPa (23 ksi). These are the highest strength levels ever achieved in an oxide dispersion strengthened alloy designed for turbine blade applications.

Effect of Grain Structure on the 1093°C (2000°F) Rupture Life. The elongated grain structure was found to have a significant effect on rupture life. Figure 11 shows

a plot of applied rupture stresses versus rupture lives for N56A and N56B bars. For the same dispersoid level, the projected 100 hour rupture life is about 131 MPa (19 ksi) for N56B, compared with about 152 MPa (22 ksi) for N56A. This increment of about 21 MPa (3 ksi) can be attributed to the difference in grain structure. Figures 12a and 12b show longitudinal sections of broken stress rupture samples of N56A-4 and N56B-1. Ideal coarse continuous elongated grains were developed in N56A-4 as shown in Figure 12a. Few secondary cracks along the transverse grain boundaries were noted. By comparison, numerous secondary transverse cracks appear in the N56B-1 (see Figure 12b) due to its poorer recrystallization response. In this case, the estimated GAR is about 7:1. This result shows that for the same dispersoid condition it is essential to have coarse elongated (GAR >10) grain structure to improve the high temperature strength.

Effect of Dispersoid Variables on the 1093°C (2000°F) Rupture Life. The control of dispersoid variables such as the volume fraction and particle size is known to be an important parameter in improving high temperature strength when a similar grain structure is achieved. Figure 13 shows a plot of rupture stress versus rupture life for bars of N39, N40, N48 and N56 taken from the data in Table VIII. Metallographic examination revealed that all the test bars had comparable elongated grains with GAR >10. A comparison, for example, of N39B and N56A is shown in Figure 14. Thus, a valid evaluation of dispersoid parameters can be made. Figure 13 shows that the 100 hour rupture stress of N39B (2.5%  $Y_2O_3$  at 35 nm diameter) is about 31 MPa (4.5 ksi) greater than that of N40B (1%  $Y_2O_3$  at 35 nm diameter). The 31 MPa (4.5 ksi) increment in rupture capability can, therefore, be attributed to the effect of  $Y_2O_3$  volume fraction.

The effect of dispersoid size can be judged by comparing N39B (2.5%  $Y_2O_3$  at 35 nm diameter) with that of N48B (2.5%  $Y_2O_3$  at 45 nm diameter). Here it is noted that increasing the  $Y_2O_3$  particle diameter to 45 nm results in a decrease in 100 hour rupture strength capability of about 21 MPa (3 ksi). Increasing the volume fraction of  $Y_2O_3$  to 4 percent at the coarser particle diameter of 45 nm (N56A) does not improve the rupture strength capability over that shown for N48B. From the above results, it would appear that a dispersoid level of 2.5 percent and  $Y_2O_3$  particles of 35 nm diameter; i.e., bar N39, is nearly optimum.

#### E. 760°C (1400°F) Stress Rupture Properties

Table IX shows the 760°C (1400°F) rupture data obtained for an applied stress of 551 MPa (80 ksi). All

test specimens were heat treated 1/2 hour/1232°C (2250°F)/AC + 24 hours/843°C (1550°F)/AC after zone annealing at 1232°C (2250°F) (standard heat treatment). While it is difficult to draw conclusions based on only a single test stress, it would appear from these results that extrusion conditions, in general, have a relatively small effect on rupture life. A low volume fraction of dispersoid (cf. N40 with N39) does appear to result in lower rupture life for a given extrusion condition. Oxide particle size (cf. N39 and N48) does not appear to affect rupture life.

The effects of different intermediate annealing prior to final aging to 843°C (1550°F) in the N39B bar on 760°C (1400°F) rupture properties were further investigated. The applied post-recrystallization heat treatments in the N39B bar is as follows:

1. 1/2 Hour/1232°C (2250°F)/AC + 24 Hours/843°C (1550°F)/AC (standard heat treatment).
2. 1/2 Hour/1232°C (2250°F)/FC to 1066°C (1950°F)/AC + 24 Hours/843°C (1550°F)/AC.
3. 1/2 Hour/1232°C (2250°F)/AC + 2 Hours/1066°C (1950°F)/AC + 24 Hours/843°C (1550°F)/AC.
4. 1/2 Hour/1232°C (2250°F)/AC + 2 Hours/954°C (1750°F)/AC + 24 Hours/843°C (1550°F)/AC.

The effect of heat treatment on  $\gamma'$  precipitation is illustrated in Figures 15 through 18. The  $\gamma'$  developed for heat treatment 1 (Figure 15) consists of a uniform distribution of precipitates approximately 0.3 $\mu$ m in diameter. With furnace cooling (Figure 16), large irregularly shaped  $\gamma'$  precipitates, about 1 $\mu$ m in diameter, formed. Upon aging at 843°C (1550°F) very fine  $\gamma'$  precipitates, about 0.08 $\mu$ m, in diameter formed between the coarse  $\gamma'$ . The structure developed for heat treatment 3 is shown in Figure 17. Here the  $\gamma'$  consists of a uniform distribution of precipitates about 0.4 $\mu$ m in diameter. The amount of background fine  $\gamma'$  is less than that produced in heat treatment 2. Figure 18 shows the  $\gamma'$  distribution produced by heat treatment 4. The  $\gamma'$  precipitates are about 0.2 $\mu$ m in diameter. Surprisingly, the  $\gamma'$  size for heat treatment 4 is somewhat less than that of heat treatment 1.

In addition to  $\gamma'$ , observations of grain boundaries showed the presence of coarse precipitates. These are assumed to be a carbide or possibly a nitride. Both  $M_{23}C_6$  and TiN were detected in extracts from samples of heat treated bar. The coarse grain boundary precipitates are



present as discrete particles. No evidence of film formation was observed.

Stress rupture data for the various heat treatments are listed in Table X. A constant stress of 551 MPa (80 ksi) was employed to determine the effect of heat treatment on rupture life and ductility. Duplicate tests were performed.

The rupture elongation (1.2%) of specimens given heat treatment 1 were lower than those for the other heat treated specimens, generally 2.5 percent. The rupture life of specimens given heat treatment 1 ranged between 87 and 148 hours. The imposition of a 1066°C (1950°F) intermediate anneal (heat treatment 3) gave lower rupture lives (80-82 hours) than those for heat treatment 1. Heat treatment 4, having the 954°C (1750°F) intermediate anneal, showed increased rupture life and elongation over those of heat treatment 1 for one specimen (N39B-4H-2). A second specimen (N39B-4H-1) gave a shorter life. This may be due to the fact that this specimen was heat treated after machining because of a previous improper heat treatment of the bar sample. The lowest rupture lives (26-45 hours) were obtained for samples furnace cooled (heat treatment 2) from 1232°C (2250°F).

The fracture profiles of tested samples of material given heat treatment 1 and heat treatment 4 are shown in Figure 19. For both treatments fracture was transgranular. Little evidence for cavitation was observed.

Although the data are limited, a comparison between  $\gamma'$  size and distribution and properties indicates that the 760°C (1400°F) rupture life is controlled by the amount of fine  $\gamma'$  (0.2 $\mu$ m size) present. This suggests that higher rupture strengths should be possible by employing aging treatments which maximize the amount of desirable fine  $\gamma'$ .

To complement these data a few additional rupture tests were performed to determine the strength capability at 1149°C (2100°F), 982°C (1800°F) and 871°C (1600°F). These data are listed in Table XI. Data for the complete range of temperatures examined are plotted in Figure 20.

In order to place the rupture capability in perspective a comparison of the 1000 hour rupture strength of alloy D was made with current and future alloys under development for advanced gas turbine engine blades. This comparison is shown in Figure 21. Mechanically alloyed alloy D shows a strength superiority over MAR M-200 + Hf above about 871°C (1600°F) and the  $\gamma/\gamma'-\delta$  eutectic alloy (Ni-20Nb-6Cr-2.5Al) above about 960°C (1760°F).

#### F. Tensile Properties of Alloy D

Tensile data for specimens given the various heat treatments studied are listed in Table XII. The effect of heat treatment on the 760°C (1400°F) tensile properties appears to be similar to that observed in the case of stress rupture at this temperature; i.e., higher strength is obtained for heat treatments which develop a fine  $\gamma'$  (0.2 $\mu$ m size) dispersion (heat treatment 4). Of significance is the large temperature sensitivity of yield and ultimate tensile strength between room temperature and 760°C (1400°F). The temperature dependence of yield and tensile strengths of alloy D is consistent with that observed for oxide dispersion strengthened WAZ-20 (ref. 8).

#### G. Oxidation and Sulfidation Resistances of Alloy D

A comparison of the oxidation resistance of alloy D containing various dispersoid levels with some conventionally cast nickel-base superalloys is shown in Table XIII. Excellent oxidation resistance is displayed for each sample of alloy D. Dispersoid size and level appear to have little significant effect on oxidation resistance. It is evident that the oxidation resistance of alloy D is superior to IN-738 and about equal to IN-100 and alloy 713LC.

Sulfidation tests were run for a period of 312 hours. Test data for alloy D containing different dispersoid sizes and levels are shown in Table XIV. No significant difference caused by dispersoid oxide size or volume fraction was noted. This table also shows data for alloy 713LC, IN-100, IN-738 and IN-792. Both IN-100 and alloy 713LC showed catastrophic attack after 48 and 168 hours respectively. Alloy D shows excellent resistance to attack and appears comparable in sulfidation resistance to IN-738 and IN-792. These latter two alloys are known to have outstanding sulfidation resistance.

#### H. Characteristics of $\gamma'$ and Oxide Dispersion in Alloy D

$\gamma'$  Phase. The phases present in alloy D were evaluated using duplicate zone annealed samples which were given heat treatment 1 [1/2 hr/1232°C (2250°F)/AC + 24 hrs/843°C (1550°F)/AC]. The weight fraction of  $\gamma'$  was determined as 39 percent. Quantitative metallographic analysis using the point counting technique revealed that the volume fraction of  $\gamma'$  was about 53-55 percent. This would suggest that some loss of  $\gamma'$  occurred during electrolytic extraction. The misfit between the  $\gamma'$  precipitate and  $\gamma$  matrix was calculated from precision measurements of the lattice parameters:

	<u><math>a_0(\gamma)</math></u>	<u><math>a_0(\gamma')</math></u>
Sample 1	3.585	3.597
Sample 2	3.587	3.583

These values gave an average  $\gamma/\gamma'$  misfit of 0.14 percent, a value which is on the lower side than those encountered in conventional superalloys (ref. 16). The chemical compositions of the  $\gamma$  and  $\gamma'$  phases were determined as follows:

$\gamma$  Phase: 25Cr/2.0Mo/4.4W/1.2Al/.13Ti/1.7Ta/Bal. Ni  
 $\gamma'$  Phase: 2.1Cr/.94Mo/7.2W/7.1Al/4.4Ti/3.6Ta/Bal. Ni

The partitioning of the elements between  $\gamma$  and  $\gamma'$  are similar to those generally observed for nickel-base alloys (ref. 13) except for W and Ta. These data indicate that there is more W in the  $\gamma'$  phase and more Ta in the  $\gamma$  phase than expected.

Oxide Dispersion. In addition to  $\gamma'$ , a mixed oxide  $Y_2O_3 \cdot Al_2O_3$  and TiN were identified as major phases present. Weaker reflections corresponding to  $\alpha-Al_2O_3$  and  $M_{23}C_6$  were also present on the x-ray diffraction patterns. The presence of  $Y_2O_3 \cdot Al_2O_3$ , and conversely the absence of  $Y_2O_3$ , is not surprising in view of similar findings on other dispersoid strengthened alloys containing both  $Y_2O_3$  and aluminum. It is likely that the initial  $Y_2O_3$  addition to the alloy combines with excess oxygen and aluminum from the matrix to form the mixed compound (ref. 14).

The size distribution of the dispersoid in an-annealed bar [zone annealed plus 1/2 hr/1232°C (2250°F)/WQ] containing different initial sizes of  $Y_2O_3$  was determined from an evaluation of 1000-1100 particle counts from transmission electron micrographs. Examples of the dispersoid distribution are shown in Figure 22. The size distributions are shown in Figures 23 and 24. The size distribution for initial  $Y_2O_3$  particles obtained by calcination at 704°C (1300°F), Figure 23, is very similar to that observed by Benjamin, et al (ref. 14) in alloy IN-853. The average volumetric dispersoid diameter was computed as 35 nm. A double peak (Figure 24) was observed in the size distribution of dispersoid in annealed bar for which  $Y_2O_3$  obtained by calcination at 1500°C (2732°F) was used for alloying. The average volumetric dispersoid diameter was computed as 45 nm in this case.

## V. CONCLUSION

The objective of this program was to develop and characterize the mechanical and corrosion behavior of an oxide dispersion strengthened nickel-base alloy designed for

advanced gas turbine blade applications. The results of this study show that an alloy containing nominally 0.05C/15Cr/2Mo/4W/4.5Al/2.5Ti/2Ta/15Zr/.01B/Bal. Ni/1.0Y<sub>2</sub>O<sub>3</sub> meets the program objectives.

Specifically the following alloy properties were obtained:

1. A 100 hour rupture strength of 165 MPa (24 ksi) and a projected 1000 hour strength of 158 MPa (23 ksi) at 1093°C (2000°F).
2. An estimated 103 MPa (15 ksi)/1000 hour life temperature capability of almost 1149°C (2100°F).
3. A 100 hour rupture strength of 551 MPa (80 ksi) at 760°C (1400°F).
4. Good oxidation resistance at 1100°C (2012°F) about equal to that of IN-100 and alloy 713LC.
5. Excellent sulfidation resistance similar to that of IN-738 and IN-792.

## VI. REFERENCES

1. Freche, J.C. and Ault, G.M.: "Progress in Advanced High Temperature Materials Technology", Proceedings of the Third International Symposium on Superalloys: Metallurgy and Manufacture, 1976, pp. 297-319.
2. Jackson, M.R., et al: "Coating for Directional Eutectics", NASA CR-134665, 1975.
3. Lemkey, F.D.: "Development of Directionally Solidified Eutectic Nickel and Cobalt Alloys", Final Report, Contract No. N66269-35-C-0129, Naval Air Systems Command, Dec. 1975.
4. Benjamin, J.S.: "Dispersion Strengthened Superalloys by Mechanical Alloying", Met. Trans., Vol. 1, Oct. 1970, pp. 2943-2951.
5. Benjamin, J.S. and Cairns, R.L.: "Elevated Temperature Mechanical Properties of a Dispersion Strengthened Superalloy", Modern Developments in Powder Metallurgy, H. Hausner, Ed., 1971, pp. 47-71.
6. Cairns, R.L. and Benjamin, J.S.: "Stress Rupture Behavior of a Dispersion Strengthened Superalloy", Jnl. Basic Engineering (Trans. ASME), Vol. 95, Jan. 1973, pp. 10-14.
7. Cairns, R.L., Curwick, L.R. and Benjamin, J.S.: "Grain Growth in Dispersion Strengthened Superalloys by Moving Zone Treatments", Met. Trans., Vol. 6A, Jan. 1975, pp. 179-188.
8. Glasgow, T.K.: "An Oxide Dispersion Strengthened Ni-W-Al Alloy with Superior High Temperature Strength", Proceedings of the Third International Symposium on Superalloys: Metallurgy and Manufacture, Sept. 1976, pp. 385-394.
9. Wilcox, B.A. and Clauer, A.H.: "The Role of Grain Size and Shape in Strengthening of Dispersion Hardened Nickel Alloys", Acta Met., Vol. 20, Mar. 1972, pp. 743-757.
10. Ansell, G.S. and Weertman, J.: "Creep of a Dispersion Hardened Aluminum Alloy", Transactions TMS-AIME, Vol. 215, Oct. 1959.
11. Allen, R.E.: "Directionally Recrystallized TD Ni-Cr", Proceedings of the Second International Symposium on Superalloys, Sept. 1972, pp. X1-X22.

12. Bergman, P.A., Sims, C.T. and Beltran, A.N.: "Development of Hot Corrosion Resistant Alloys for Marine Gas Turbine Service", ASTM STP 421, 1967, p. 43.

13. Kreige, O.H. and Baris, J.M.: "The Chemical Partitioning of Elements in Gamma Prime Separated from Precipitation-Hardened, High Temperature Nickel-Base Alloys", Trans. ASM, Vol. 62, 1969, pp. 195-200.

14. Benjamin, J.S., Volin, T.E. and Weber, J.H.: "Dispersoids in Mechanically Alloyed Superalloys", High Temperatures-High Pressures, Vol. 6, 1974, pp. 443-446.

15. Ashbrook, R.L.: "Directionally Solidified Composite Systems Under Evaluation", AGARD Conference Proceedings, No. 156, E.R. Thompson and P.R. Sahm Eds., 1974, pp. 93-101.

16. Decker, R.F. and Mihalisin, J.R.: "Coherency Strains in  $\gamma'$  Hardened Nickel Alloys", Trans. ASM, Vol. 62, 1969, pp. 481-489.

TABLE I  
COMPOSITION (WT. %) OF ALLOYS

<u>Alloy</u>	<u>Cr</u>	<u>Mo</u>	<u>W</u>	<u>Al</u>	<u>Ti</u>	<u>Ta</u>	<u>B</u>	<u>Zr</u>	<u>Ni</u>	<u>Y<sub>2</sub>O<sub>3</sub></u>	<u>C</u>	<u>O</u>	<u>N</u>
A	16	3	10	4.5	2.5	3	.01	.15	Bal.	1.0	.059	.66	.098
B	16	3	6	4.5	2.5	5	.01	.15	Bal.	1.0	.053	.62	.080
C	13	3	10	4.5	2.5	5	.01	.15	Bal.	1.0	.055	.62	.069
D	15	2	4	4.5	2.5	2.5	.01	.15	Bal.	1.1	.053	.67	.18

TABLE II

POWDER CHARACTERIZATION OF ALLOYS

Powder Batch	Alloy	Screen Analysis, %							
		+45	-45/+80	-80/+100	-100/+140	-140/+200	-200/+230	-230/+325	-325
N1	A	3.1	13.5	11.9	23.4	26.4	6.9	7.4	7.4
N2	A	1.8	9.1	7.5	16.4	19.2	10.1	14.5	21.4
N3	B	1.9	11.1	6.5	14.1	21.9	9.5	13.7	21.3
N4	C	0.8	7.7	4.7	14.2	23.3	10.5	15.6	23.2



TABLE III

SCREEN ANALYSIS OF ATTRITED POWDER ALLOY A

<u>Powder Batch</u>	<u>-30/+40</u>	<u>-40/+80</u>	<u>-80/+100</u>	<u>-100/+200</u>	<u>-200/+325</u>	<u>-325</u>
N11	1.0	9.6	5.9	36.4	24.4	22.7
N12	0.6	7.1	4.1	33.5	28.9	26.3
N13	1.2	13.1	6.9	37.0	24.3	17.5
N14	2.0	10.8	9.5	50.3	16.3	11.0
N16	5.9	53.2	13.4	24.1	2.9	0.5
N17	3.7	17.6	7.4	32.0	22.4	16.9
N18	2.2	16.4	8.8	29.2	21.2	22.2
N19	2.2	16.4	5.6	32.2	21.7	21.9
N20	3.6	22.3	7.3	25.1	17.8	23.9
N21	2.6	16.1	6.9	29.7	20.1	24.6
N22	1.7	17.5	6.8	28.6	20.8	24.6

ORIGINAL PAGE IS  
OF POOR QUALITY

TABLE IV  
EFFECT OF EXTRUSION CONDITIONS ON GRAIN STRUCTURE OF ALLOY A

Bar	Extrusion Conditions				Structure			
	Temperature	Ratio	Ram Speed		Conventional Anneal		Zone Anneal	
			cm/sec	(in/sec)	Description	GAR	Description	GAR
N23A	1093°C (2000°F)	16:1	17.0	(6.7)	Partial Rx	—	Not Annealed	
N23B	1093°C (2000°F)	22:1		(N.R.)	Partial Rx	—	Not Annealed	
N23C	1093°C (2000°F)	12:1	6.7	(6.6)	Partial Rx	—	Not Annealed	
N23D	1066°C (1950°F)	12:1	20.6	(8.1)	Partial Rx	—	Partial Rx	
N23E	1066°C (1950°F)	16:1	18.0	(7.1)	Partial Rx	—	Partial Rx	
N23F	1066°C (1950°F)	22:1	15.0	(5.9)	Partial Rx	—	Partial Rx	
N23G	1038°C (1900°F)	12:1	17.3	(6.8)	Mixed C.El. and M.Eq.	2.6	Partial Rx	
N23H	1038°C (1900°F)	16:1	15.5	(6.1)	Mixed C.El. and M.Eq.	5.0	C.El.	Approx. 7:1
N23I	1038°C (1900°F)	22:1	12.4	(4.9)	C.El.	8.1	C.El.	Approx. 5:1
N23J	1038°C (1900°F)	22:1	4.1	(1.6)	C.El.*	6.9	Partial Rx	
N23K	1038°C (1900°F)	16:1		(N.R.)	Partial Rx	—	Partial Rx	
N23L	1038°C (1900°F)	12:1		(N.R.)	Partial Rx	—		
N23M	1066°C (1950°F)	22:1	5.3	(2.1)	C.El.*	5.6	C.El.	Approx. 6:1
N23N	1066°C (1950°F)	16:1	5.1	(2.0)	Partial Rx	—	Not Annealed	
N23O	1066°C (1950°F)	12:1	4.3	(1.7)	Partial Rx	—	Not Annealed	
N23P	1093°C (2000°F)	22:1		(N.R.)	Partial Rx	—	Not Annealed	
N23Q	1093°C (2000°F)	16:1	5.3	(2.1)	Partial Rx	—	Not Annealed	
N23R	1093°C (2000°F)	12:1	5.8	(2.3)	Partial Rx	—	Not Annealed	

C.El. - Coarse elongated grains.

M.Eq. - C.Eq.: medium to coarse equiaxed grains.

\* - Occasional stringers of unrecrystallized grains.

Rx - Recrystallization.

GAR - Ratio of grain length to grain diameter.

TABLE V

1093°C (2000°F) STRESS RUPTURE DATA

Bar No.	Extrusion Conditions					Stress		Life (hr)	% Elong.	% R.A.
	Temperature	Ratio	Ram Speed		MPa	(ksi)				
			cm/sec	(in/sec)						
(a) <u>Conventionally Annealed Bar</u>										
N23D-45	1066°C (1950°F)	12:1	20.6	(8.1)	97	(14)	0	8.0	5.6	
N23E-45	1066°C (1950°F)	16:1	18.0	(7.1)	97	(14)	0	6.4	4.7	
N23F-45	1066°C (1950°F)	22:1	15.0	(5.9)	97	(14)	0	4.0	3.1	
N23G-45	1038°C (1900°F)	12:1	17.3	(6.8)	97	(14)	4.1	Nil	Nil	
N23H-45	1038°C (1900°F)	16:1	15.5	(6.1)	97	(14)	2.4	UNBROKEN		
					110	(16)	10.4	Nil	Nil	
N23I-45	1038°C (1900°F)	22:1	12.4	(4.9)	97	(14)	3.7	THREAD FAILURE		
N23I-44	1038°C (1900°F)	22:1	12.4	(4.9)	97	(14)	24	UNBROKEN		
					110	(16)	7.3	1.6	0.8	
N23J-45	1038°C (1900°F)	22:1	4.1	(1.6)	97	(14)	24	UNBROKEN		
					110	(16)	7.7	1.6	Nil	
N23K-45	1038°C (1900°F)	16:1	4.6	(1.8) [Est.]	97	(14)	0	0.8	Nil	
N23M-45	1066°C (1950°F)	22:1	5.1	(2.0) [Est.]	97	(14)	23.4	1.6	Nil	
(b) <u>Zone Annealed Bar</u>										
N23G-42	1038°C (1900°F)	12:1	15.0	(5.9)	97	(14)	0.5	1.3	1.5	
N23H-42	1038°C (1900°F)	16:1	15.5	(6.1)	97	(14)	23.4	2.5	Nil	
N23J-42	1038°C (1900°F)	22:1	12.4	(4.9)	97	(14)	15.4	Nil	Nil	
N23M-42	1066°C (1950°F)	22:1	5.1	(2.0) [Est.]	97	(14)	0	116	81.2	

TABLE VI

SCREEN ANALYSIS OF POWDER BLENDS OF ALLOY D

<u>Blend</u>	<u>Dispersoid</u>		<u>+40</u>	<u>-40/+100</u>	<u>-100/+200</u>	<u>-200/+325</u>	<u>-325</u>
	<u>Vol. %</u>	<u>Size</u>					
N39	2.5	35 nm	3.4	46.2	31.4	11.7	6.6
N40	1.0	35 nm	6.5	68.2	20.0	3.6	1.8
N48	2.5	45 nm	10.8	54.0	23.0	6.5	5.0
N56	4.0	45 nm	5.8	29.6	34.8	17.4	12.4

TABLE VII  
EXTRUSION VARIABLES

<u>Extrusions</u>	<u>Temperature</u>	<u>Ratio</u>	<u>Ram Speed</u>	
			<u>cm/sec</u>	<u>(in/sec)</u>
N39A, N40A, N48A, N56A	1038°C (1900°F)	16:1	7.6	3
N39B, N40B, N48B, N56B	1038°C (1900°F)	16:1	20.3	8
N39C, N40C, N49C, N56C	1038°C (1900°F)	20:1	7.6	3
N39D, N40D, N49D, N56D	1038°C (1900°F)	20:1	20.3	8
N39E, N40E, N49E, N56E	1093°C (2000°F)	16:1	7.6	3
N39F, N40F, N49F, N56F	1093°C (2000°F)	16:1	20.3	8
N39G, N40G, N49G, N56G	1093°C (2000°F)	20:1	7.6	3
N39H, N40H, N49H, N56H	1093°C (2000°F)	20:1	20.3	8

TABLE VIII

1093°C (2000°F) STRESS RUPTURE DATA

Specimen No.	Extrusion Conditions					Stress		Life (hrs)	% Elong.	% R.A.
	Ratio	Temperature	Ram Speed			MPa	(ksi)			
			cm/sec	(in/sec)						
(a) ALLOY N39 (35 nm Y <sub>2</sub> O <sub>3</sub> PARTICLES AT 2.5 VOLUME PERCENT)										
N39A-1	16:1	1038°C (1900°F)	7.6	(3)		172	(25)	9.1	2.5	4.3
N39A-2	16:1	1038°C (1900°F)	7.6	(3)		172	(25)	3.9	1.3	4.4
N39A-5	16:1	1038°C (1900°F)	7.6	(3)		165	(24)	19.7	2.5	1.5
N39B-1	16:1	1038°C (1900°F)	20.3	(8)		152	(22)	24+	UNBROKEN	
						165	(24)	24+	UNBROKEN	
						179	(26)	2.2	2.5	8.3
N39B-2	16:1	1038°C (1900°F)	20.3	(8)		172	(25)	44.0	2.5	8.3
N39B-3	16:1	1038°C (1900°F)	20.3	(8)		172	(25)	38.0	2.5	8.7
N39B-5	16:1	1038°C (1900°F)	20.3	(8)		165	(24)	149.4	2.5	4.3
N39C-1	20:1	1038°C (1900°F)	7.6	(3)		172	(25)	12.1	2.5	8.7
N39C-2	20:1	1038°C (1900°F)	7.6	(3)		172	(25)	13.9	2.5	7.3
N39C-5	20:1	1038°C (1900°F)	7.6	(3)		165	(24)	28.9	1.3	1.5
N39D-1	20:1	1038°C (1900°F)	20.3	(8)		172	(25)	1.6	5.0	8.7
N39D-3	20:1	1038°C (1900°F)	20.3	(8)		172	(25)	1.8	7.5	11.4
N39E-1	16:1	1093°C (2000°F)	7.6	(3)		172	(25)	0.2	2.5	2.9
N39E-2	16:1	1093°C (2000°F)	7.6	(3)		165	(24)	0.6	2.5	5.8
N39F-1	16:1	1093°C (2000°F)	20.3	(8)		172	(25)	0.5	3.8	7.1
N39F-2	16:1	1093°C (2000°F)	20.3	(8)		165	(24)	0.6	2.5	8.6
N39G-1	20:1	1093°C (2000°F)	7.6	(3)		172	(25)	0.4	3.8	8.7
N39G-2	20:1	1093°C (2000°F)	7.6	(3)		165	(24)	0.8	3.7	8.8
N39H-1	20:1	1093°C (2000°F)	20.3	(8)		172	(25)	0.6	2.5	7.1
N39H-2	20:1	1093°C (2000°F)	20.3	(8)		165	(24)	1.0	3.7	5.8
N39B-3	16:1	1038°C (1900°F)	20.3	(8)		172	(25)	38.0	2.5	8.7
N39B-5	15:1	1038°C (1900°F)	20.3	(8)		165	(24)	149.4	2.5	4.3

TABLE VIII (CONTINUED)

Specimen No.	Extrusion Conditions				Stress		Life	% Elong.	% R.A.
	Ratio	Temperature	Ram Speed cm/sec	(in/sec)	MPa	(ksi)	(hrs)		
(b) ALLOY N40 (35 nm Y <sub>2</sub> O <sub>3</sub> PARTICLES AT 1.0 VOLUME PERCENT)									
N40A-1	16:1	1038°C (1900°F)	7.6	(3)	152	(22)	3.1	5.0	5.8
N40A-2	16:1	1038°C (1900°F)	7.6	(3)	152	(22)	3.7	2.5	9.9
N40A-3	16:1	1038°C (1900°F)	7.6	(3)	139	(20)	19.1	1.3	4.3
N40A-4	16:1	1038°C (1900°F)	7.6	(3)	139	(20)	24.7	2.5	2.9
N40B-1	16:1	1038°C (1900°F)	20.3	(8)	152	(22)	20.8	2.5	7.3
N40B-2	16:1	1038°C (1900°F)	20.3	(8)	152	(22)	2.6	2.5	4.3
N40B-3	16:1	1038°C (1900°F)	20.3	(8)	139	(20)	50.5	3.8	4.3
N40B-6	16:1	1038°C (1900°F)	20.3	(8)	139	(20)	71.6	2.5	0.8
N40C-1	20:1	1038°C (1900°F)	7.6	(3)	152	(22)	7.7	3.7	14.2
N40C-2	20:1	1038°C (1900°F)	7.6	(3)	152	(22)	2.8	5.0	11.5
N40C-3	20:1	1038°C (1900°F)	7.6	(3)	139	(20)	30.5	3.8	9.9
N40C-4	20:1	1038°C (1900°F)	7.6	(3)	139	(20)	51.0	2.5	7.1
N40D-1	20:1	1038°C (1900°F)	20.3	(8)	139	(20)	160.5	1.3	1.5
N40D-2	20:1	1038°C (1900°F)	20.3	(8)	152	(22)	10.4	3.5	5.8
N40E-1	16:1	1093°C (2000°F)	7.6	(3)	152	(22)	0.8	2.5	7.3
N40F	16:1	1093°C (2000°F)	20.3	(8)	152	(22)	1.8	2.5	5.8
N40G	20:1	1093°C (2000°F)	7.6	(3)	152	(22)	1.7	2.5	5.8
N40H-1	20:1	1093°C (2000°F)	20.3	(8)	152	(22)	8.1	2.5	2.9

TABLE VIII (CONTINUED)

Specimen No.	Extrusion Conditions				Stress		Life (hrs)	% Elong.	% R.A.
	Ratio	Temperature	Ram Speed		MPa	(ksi)			
			cm/sec	(in/sec)					
(c) ALLOY N48 (45 nm Y <sub>2</sub> O <sub>3</sub> PARTICLES AT 2.5 VOLUME PERCENT)									
N48A-1	16:1	1038°C (1900°F)	7.6	(3)	152	(22)	54.8	2.5	2.9
N48A-2	16:1	1038°C (1900°F)	7.6	(3)	152	(22)	39.8	3.8	5.8
N48B-1	16:1	1038°C (1900°F)	20.3	(8)	152	(22)	24+	UNBROKEN	
					165	(24)*	27.8		
N48B-2	16:1	1038°C (1900°F)	20.3	(8)	152	(22)	34.2	1.3	4.4
N48B-3	16:1	1038°C (1900°F)	20.3	(8)	152	(22)	63.1	3.8	11.3
N48C-1	20:1	1038°C (1900°F)	7.6	(3)	165	(24)*	0.4	1.3	4.3
N48C-2	20:1	1038°C (1900°F)	7.6	(3)	152	(22)	10.6	2.5	4.4
N48D-1	20:1	1038°C (1900°F)	20.3	(8)	152	(22)	56.0	3.7	7.2
N48D-2	20:1	1038°C (1900°F)	20.3	(8)	165	(24)	12.4	2.7	5.8
N48E-1	16:1	1093°C (2000°F)	7.6	(3)	165	(24)	0.3	3.8	7.0
N48E-2	16:1	1093°C (2000°F)	7.6	(3)	152	(22)	0.6	2.5	1.5
N48F-1	16:1	1093°C (2000°F)	20.3	(8)	165	(24)	0.3	2.5	7.8
N48F-2	16:1	1093°C (2000°F)	20.3	(8)	152	(22)	0.5	2.5	7.2
N48G-1	20:1	1093°C (2000°F)	7.6	(3)	165	(24)	1.1	3.8	8.4
N48G-2	20:1	1093°C (2000°F)	7.6	(3)	152	(22)	2.0	5.0	5.7
N48H-1	20:1	1093°C (2000°F)	20.3	(8)	165	(24)	0.5	5.0	8.5
N48H-2	20:1	1093°C (2000°F)	20.3	(8)	152	(22)	3.5	3.7	8.5

\*Step load test.



TABLE VIII (CONTINUED)

Specimen No.	Extrusion Conditions				Stress		Life (hrs)	% Elong.	% R.A.
	Ratio	Temperature	Ram Speed		MPa	(ksi)			
			cm/sec	(in/sec)					
(d) ALLOY N56 (45 nm Y <sub>2</sub> O <sub>3</sub> PARTICLES AT 4.0 VOLUME PERCENT)									
N56A-1	16:1	1038°C (1900°F)	7.6	(3)	152	(22)	24+	UNBROKEN	
					165	(24)*	2.6	3.8	12.4
N56A-2	16:1	1038°C (1900°F)	7.6	(3)	165	(24)	4.7	3.8	11.4
N56A-3	16:1	1038°C (1900°F)	7.6	(3)	152	(22)	48.4	3.8	10.0
N56A-4	16:1	1038°C (1900°F)	7.6	(3)	152	(22)	84.7	2.5	5.7
N56B-1	16:1	1038°C (1900°F)	20.3	(8)	152	(22)	1.6	2.5	4.3
N56B-2	16:1	1038°C (1900°F)	20.3	(8)	152	(22)	1.2	2.5	2.9
N56B-3	16:1	1038°C (1900°F)	20.3	(8)	139	(20)	7.8	2.5	4.4
N56B-4	16:1	1038°C (1900°F)	20.3	(8)	139	(20)	4.6	2.5	4.4
N56C-1	20:1	1038°C (1900°F)	7.6	(3)	152	(22)	99.2	2.5	5.9
N56C-2	20:1	1038°C (1900°F)	7.6	(3)	165	(24)	19.3	2.7	5.8
N56D-1	20:1	1038°C (1900°F)	20.3	(8)	139	(20)	6.2	1.3	3.0
N56D-3	20:1	1038°C (1900°F)	20.3	(8)	152	(22)	0.7	1.3	4.4
N56E-1	16:1	1093°C (2000°F)	7.6	(3)	152	(22)	0.4	3.8	7.1
N56F-1	16:1	1093°C (2000°F)	20.3	(8)	152	(22)	0.1	2.5	4.4
N56G-1	20:1	1093°C (2000°F)	7.6	(3)	152	(22)	0	3.7	6.2
N56G-2	20:1	1093°C (2000°F)	7.6	(3)	139	(20)	0	3.8	5.8
N56G-3	20:1	1093°C (2000°F)	7.6	(3)	124	(18)	2.3	2.5	2.9
N56H-1	20:1	1093°C (2000°F)	20.3	(8)	152	(22)	3.7	6.2	3.0

\*Step load test.

TABLE IX

760°C (1400°F) STRESS RUPTURE DATA

Specimen No.	Extrusion Conditions				Stress		Life (hrs)	% Elong.	% R.A.
	Ratio	Temperature	Ram Speed		MPa	(ksi)			
			cm/sec	(in/sec)					
(a) ALLOY N39 (35 nm Y <sub>2</sub> O <sub>3</sub> PARTICLES AT 2.5 VOLUME PERCENT)									
N39A-3	16:1	1038°C (1900°F)	7.6	(3)	551	(80)	68.8	1.3	2.9
N39A-4	16:1	1038°C (1900°F)	7.6	(3)	586	(85)	48.5	1.3	5.9
N39B-3	16:1	1038°C (1900°F)	20.3	(8)	551	(80)	100.7	1.3	5.7
N39C-3	20:1	1038°C (1900°F)	7.6	(3)	551	(80)	93.1	1.3	5.8
N39D-2	20:1	1038°C (1900°F)	20.3	(8)	551	(80)	93.0	1.3	4.4
N39E-3	16:1	1093°C (2000°F)	7.6	(3)	551	(80)	38.5	3.7	4.4
N39F-3	16:1	1093°C (2000°F)	20.3	(8)	551	(80)	29.0	2.5	5.7
N39G-3	20:1	1093°C (2000°F)	7.6	(3)	551	(80)	49.4	2.5	4.6
N39G-3	20:1	1093°C (2000°F)	20.3	(8)	551	(80)	34.3	3.7	7.0
(b) ALLOY N40 (35 nm Y <sub>2</sub> O <sub>3</sub> PARTICLES AT 1.0 VOLUME PERCENT)									
N40A-5	16:1	1038°C (1900°F)	7.6	(3)	551	(80)	50.1	2.5	7.2
N40B-5	16:1	1038°C (1900°F)	20.3	(8)	551	(80)	57.2	1.3	Nil
N40C-5	20:1	1038°C (1900°F)	7.6	(3)	551	(80)	73.1	1.3	4.4
N40D-3	20:1	1038°C (1900°F)	20.3	(8)	551	(80)	18.5	4.3	2.5
N40E-2	16:1	1093°C (2000°F)	7.6	(3)	551	(80)	22.0	2.5	5.9
N40F-2	16:1	1093°C (2000°F)	20.3	(8)	551	(80)	28.0	2.5	5.8
N40G-2	20:1	1093°C (2000°F)	7.6	(3)	551	(80)	70.5	2.5	5.8
N40H-2	20:1	1093°C (2000°F)	20.3	(8)	551	(80)	22.4	2.5	4.3

TABLE IX (CONTINUED)

Specimen No.	Extrusion Conditions				Stress		Life	% Elong.	% R.A.
	Ratio	Temperature	Ram Speed		MPa	(ksi)	(hrs)		
			cm/sec	(in/sec)					
(c) ALLOY N48 (45 nm Y <sub>2</sub> O <sub>3</sub> PARTICLES AT 2.5 VOLUME PERCENT)									
N48A-3	16:1	1038°C (1900°F)	7.6	(3)	551	(80)	93.7	1.3	7.3
N48B-4	16:1	1038°C (1900°F)	20.3	(8)	551	(80)	84.0	2.5	4.4
N48C	20:1	1038°C (1900°F)	7.6	(3)	NO TEST				
N48D-3	20:1	1038°C (1900°F)	20.3	(8)	551	(80)	44.5	2.5	5.7
N48E-3	16:1	1093°C (2000°F)	7.6	(3)	551	(80)	80.4	3.8	4.3
N48F-3	16:1	1093°C (2000°F)	20.3	(8)	551	(80)	51.6	2.5	3.0
N48G-3	20:1	1093°C (2000°F)	7.6	(3)	551	(80)	75.9	3.8	5.8
N48H-3	20:1	1093°C (2000°F)	20.3	(8)	551	(80)	64.9	1.3	1.4
(d) ALLOY N56 (45 nm Y <sub>2</sub> O <sub>3</sub> PARTICLES AT 4.0 VOLUME PERCENT)									
N56A-5	16:1	1038°C (1900°F)	7.6	(3)	551	(80)	104.0	1.3	2.9
N56B-5	16:1	1038°C (1900°F)	20.3	(8)	551	(80)	20.3	2.5	5.7
N56C-3	20:1	1038°C (1900°F)	7.6	(3)	551	(80)	37.0	3.7	8.6
N56D-2	20:1	1038°C (1900°F)	20.3	(8)	551	(80)	16.1	1.3	1.6
N56E-2	16:1	1093°C (2000°F)	7.6	(3)	551	(80)	24.4	3.8	3.5
N56F-2	16:1	1093°C (2000°F)	20.3	(8)	551	(80)	8.9	2.5	4.3
N56G-3	20:1	1093°C (2000°F)	7.6	(3)	551	(80)	12.5	2.5	4.3
N56H-2	20:1	1093°C (2000°F)	20.3	(8)	551	(80)	31.5	1.3	Nil

TABLE X  
EFFECT OF HEAT TREATMENT ON  
760°C (1400°F) RUPTURE PROPERTIES

<u>Specimen No.</u>	<u>Heat Treatment</u>	<u>Stress</u>		<u>Life (hrs)</u>	<u>% Elong.</u>	<u>% R.A.</u>
		<u>MPa</u>	<u>(ksi)</u>			
N39B-1H-1	1	551	(80)	148.0	1.2	4.5
N39B-1H-2	1	551	(80)	87.4	1.2	9.5
N39B-1H-4 <sup>a</sup>	1	551	(80)	100.7	1.3	5.7
N39B-2H-1	2	551	(80)	45.0	2.5	5.9
N39B-2H-2	2	551	(80)	26.6	2.5	4.3
N39B-3H-1	3	551	(80)	82.4	1.2	8.5
N39B-3H-2	3	551	(80)	80.0	2.5	8.5
N39B-4H-1 <sup>b</sup>	4	551	(80)	74.9	2.5	4.5
N39B-4H-2	4	551	(80)	168.5	2.5	2.8

<sup>a</sup>From previous test.

<sup>b</sup>This specimen only heat treated after machining.

Heat Treatment

- 1 - Zone Anneal + 1/2 hr/1232°C (2250°F)/AC + 24 hrs/843°C (1550°F)/AC
- 2 - Zone Anneal + 1/2 hr/1232°C (2250°F)/FC to 1066°C (1950°F)/AC + 2 hrs/843°C (1550°F)/AC
- 3 - Zone Anneal + 1/2 hr/1232°C (2250°F)/AC + 2 hrs/1066°C (1950°F)/AC + 24 hrs/843°C (1550°F)/AC
- 4 - Zone Anneal + 1/2 hr/1232°C (2250°F)/AC + 2 hrs/954°C (1750°F)/AC + 24 hrs/843°C (1550°F)/AC

TABLE XI  
STRESS RUPTURE DATA

<u>Sample No.</u>	<u>Test Temperature</u>	<u>Stress</u>		<u>Life</u> (hrs)	<u>% Elong.</u>	<u>% R.A.</u>
		<u>MPa</u>	<u>(ksi)</u>			
N39I-1	1149°C (2100°F)	152	(22)	0.1	5.0	15.5
N39I-2	1149°C (2100°F)	138	(20)	6.2	2.5	5.8
N39I-3	1149°C (2100°F)	124	(18)	32.7	2.5	2.9
N39I-4	1149°C (2100°F)	110	(16)	149.7	3.8	5.8
N48B-5	982°C (1800°F)	220	(32)	5.1	2.5	3.0
N48B-6	982°C (1800°F)	220	(32)	57.5	3.8	5.0
N48B-7	982°C (1800°F)	193	(28)	476.7	Nil	Nil
N40C-3	871°C (1600°F)	276	(40)*	258	UNBROKEN	
		345	(50)	42.2	2.5	3.0
N40C-4	871°C (1600°F)	310	(45)	246.4	2.5	5.8

\*Step load test.

NOTE: Bar N39I was extruded under same conditions as N39B and gave essentially the same grain structure upon zone annealing.

TABLE XII  
TENSILE TEST DATA

<u>Sample No.</u>	<u>Heat Treatment</u>	<u>Test Temperature</u>	<u>0.2% Y.S.</u>		<u>U.T.S.</u>		<u>% Elong.</u>	<u>% R.A.</u>
			<u>MPa</u>	<u>(ksi)</u>	<u>MPa</u>	<u>(ksi)</u>		
N39B-1T	1	RT	1275	(185.1)	1284	(186.4)	2.0	6.0
N39B-7T	2	RT	1245	(180.7)	1290	(187.3)	2.0	5.0
N39B-2T	1	760°C (1400°F)	881	(127.9)	891	(129.3)	3.5	10.0
N39B-4T	2	760°C (1400°F)	854	(124.0)	896	(130.0)	3.5	8.5
N39B-5T	3	760°C (1400°F)	851	(123.5)	923	(134.0)	3.5	6.0
N39B-6T	4	760°C (1400°F)	902	(130.9)	923	(133.9)	3.5	7.5
N39C-3T	1	1093°C (2000°F)	216	( 31.3)	249	( 36.1)	5.5	21.0

Heat Treatment

- 1 - Zone Anneal + 1/2 hr/1232°C (2250°F)/AC + 24 hrs/ 843°C (1550°F)/AC
- 2 - Zone Anneal + 1/2 hr/1232°C (2250°F)/FC to 1066°C (1950°F)/AC + 24 hrs/843°C (1550°F)/AC
- 3 - Zone Anneal + 1/2 hr/1232°C (2250°F)/AC + 24 hrs/1066°C (1950°F)/AC + 24 hrs/843°C (1550°F)/AC
- 4 - Zone Anneal + 1/2 hr/1232°C (2250°F)/AC + 2 hrs/ 954°C (1750°F)/AC + 24 hrs/843°C (1550°F)/AC

TABLE XIII

1100°C (2012°F) CYCLIC OXIDATION RESISTANCE

<u>Alloy</u>	<u>Condition</u>	<u>Wt. Change (mg/cm<sup>2</sup>)</u>	
		<u>Underscaled</u>	<u>Descaled</u>
Alloy D (N39A)	(1)	-12.27	-13.18
Alloy D (N40A)	(1)	- 8.29	- 9.71
Alloy D (N48A)	(1)	-16.05	-17.67
Alloy D (N56A)	(1)	-15.03	-16.40
IN-100	As-Cast	- 2.99	- 7.27
Alloy 713LC	As-Cast	-21.25	-22.08
IN-738	(2)	-45.56	-49.51

(1) Zone Annealed + 1/2 hr/1232°C (2250°F)/AC +  
24 hrs/843°C (1550°F)/AC

(2) 2 hrs/1121°C (2050°F)/AC + 24 hrs/843°C  
(1550°F)/AC

TABLE XIV

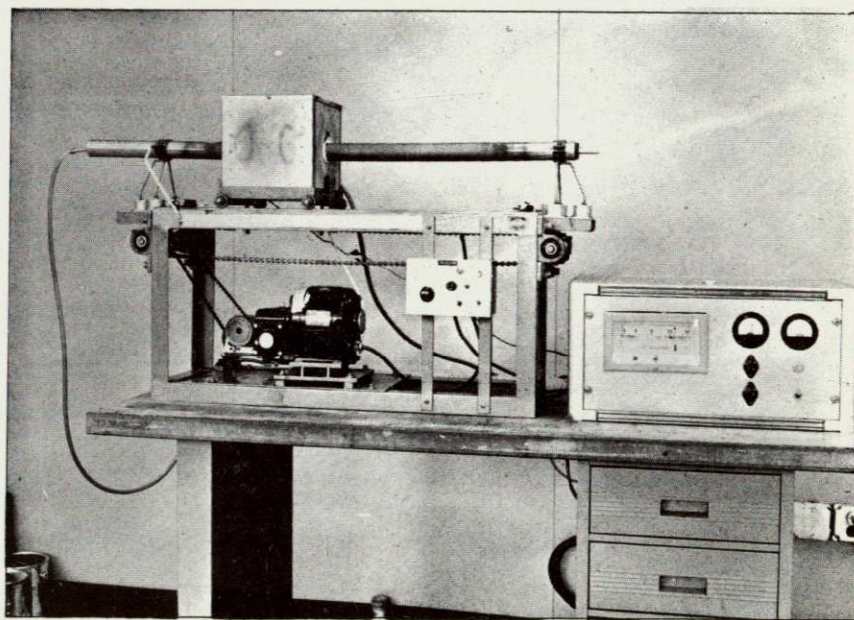
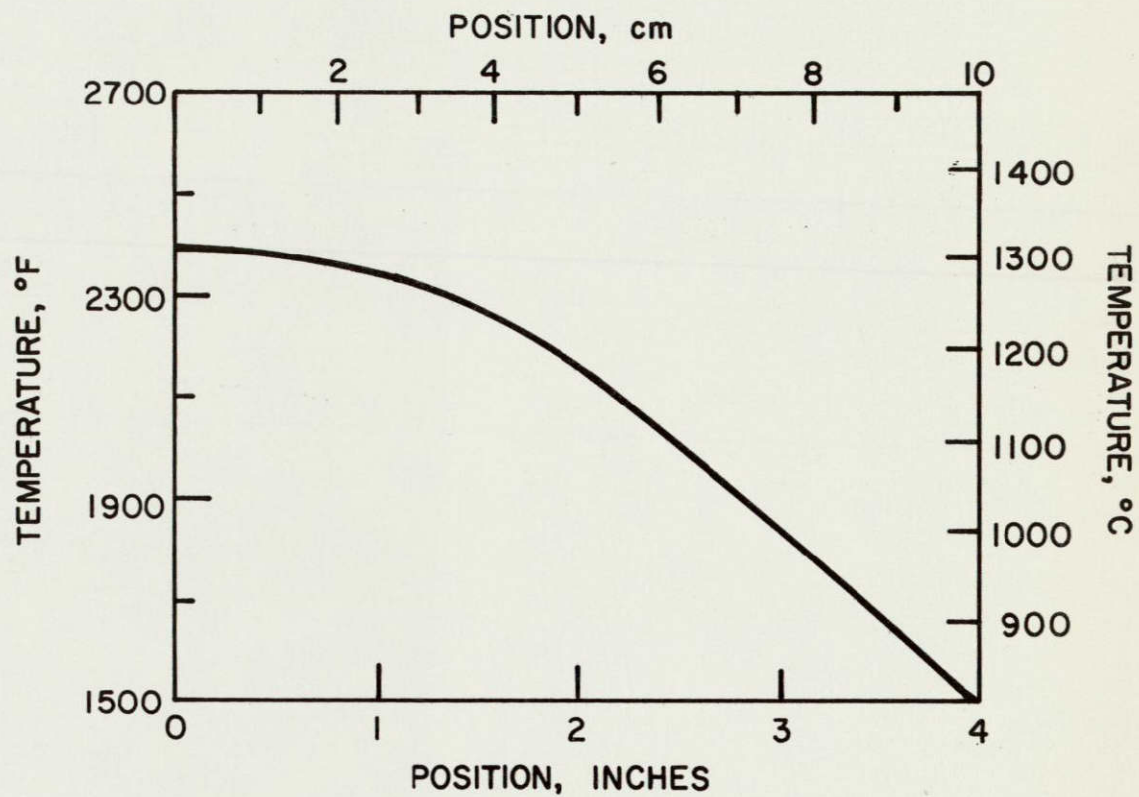
927°C (1700°F) SULFIDATION RESISTANCE

<u>Alloy</u>	<u>Exposure Time (hrs)</u>	<u>Condition</u>	<u>ΔW Undescaled (mg/cm<sup>2</sup>)</u>	<u>ΔW Descaled (mg/cm<sup>2</sup>)</u>	<u>Max. Attack (cm)</u>
Alloy D (N39A)	312	(1)	1.73	- 9.87	.0152
Alloy D (N40A)	312	(1)	1.97	- 9.10	.0259
Alloy D (N48A)	312	(1)	7.50	- 12.96	.0317
Alloy D (N56A)	312	(1)	4.15	- 12.49	.0213
IN-100	48	As-Cast	-355.29	-367.36	.1692
713LC	168	As-Cast	-410.74	-488.63	.3277
IN-738	312	(2)	4.818	- 9.73	.0157
IN-792	312	(2)	5.160	- 6.85	.0284

(1) Zone annealed + 1/2 hr/1232°C (2250°F)/AC + 24 hrs/843°C (1550°F)/AC.

(2) 2 hrs/1121°C (2050°F)/AC + 24 hrs/843°C (1550°F)/AC.

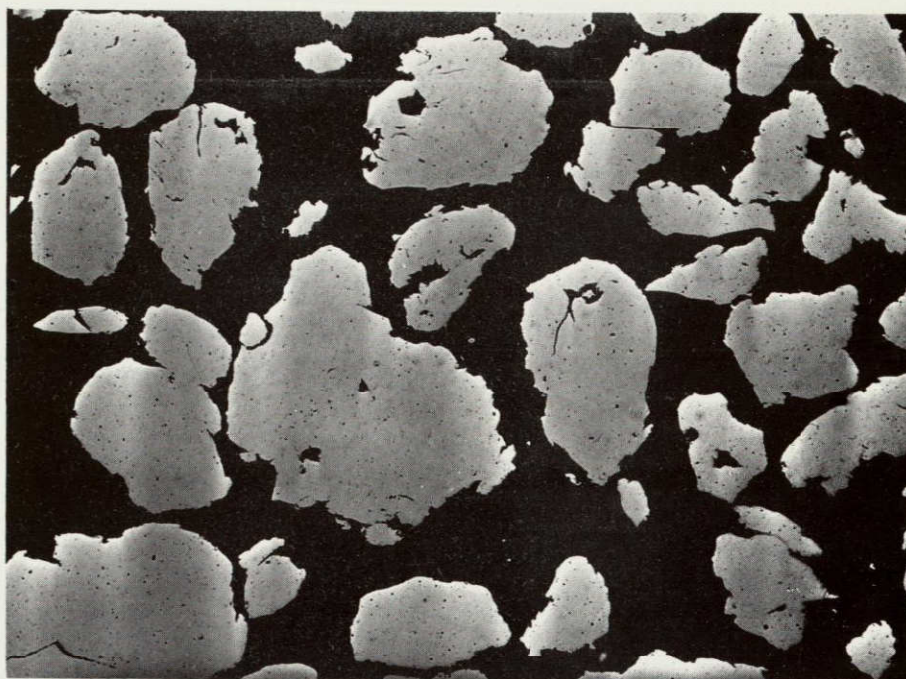




G.A. 537

FIGURE 1

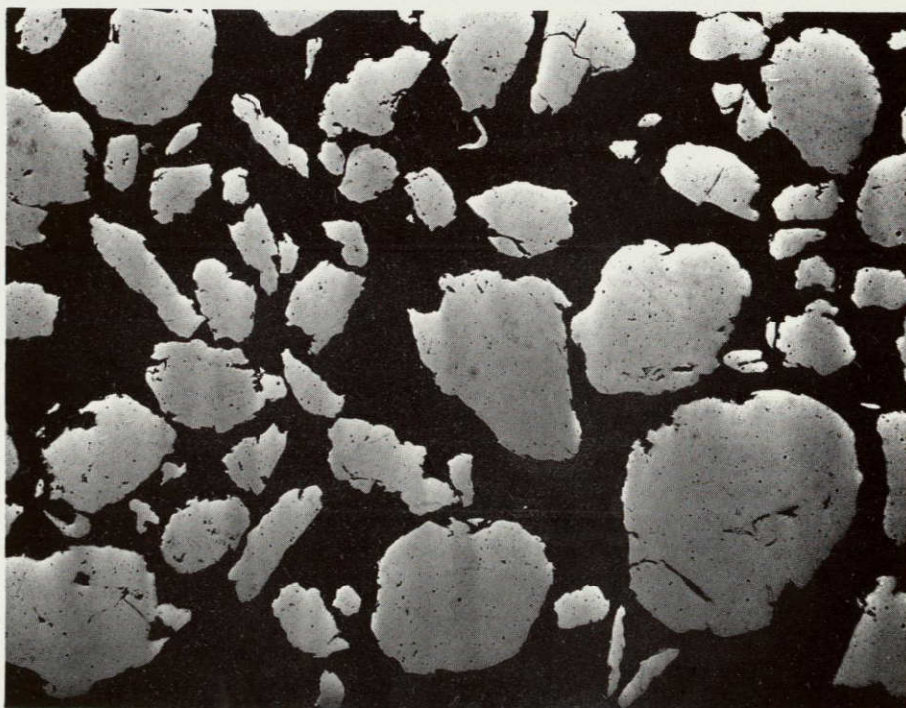
TEMPERATURE PROFILE AND FURNACE USED FOR  
GRADIENT AND ZONE ANNEALING



P.N. 1-48511

(a) Alloy A - Powder Batch N1

40 $\mu$ m



P.N. 1-48505

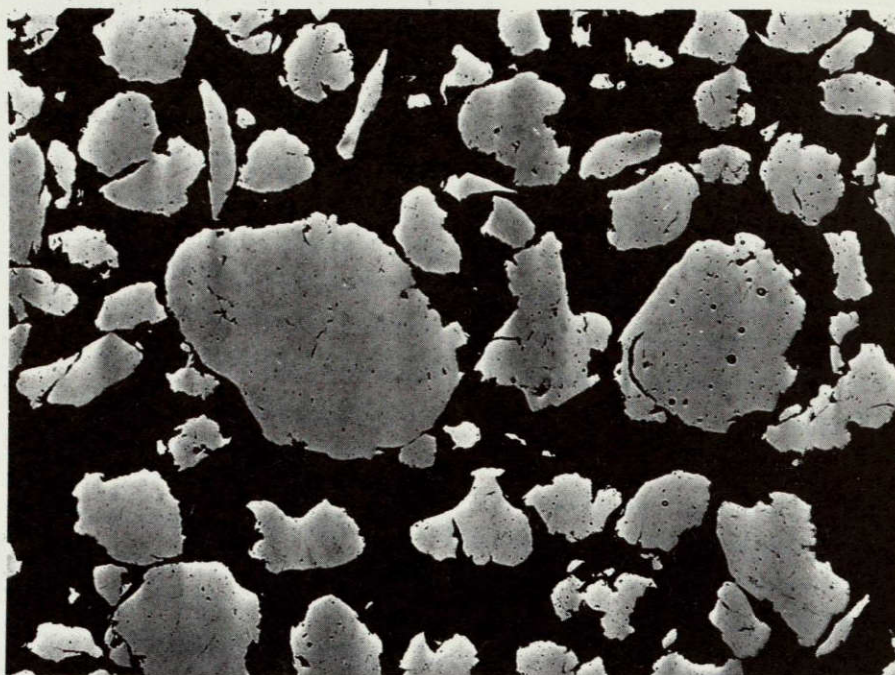
(b) Alloy A - Powder Batch N2

40 $\mu$ m

# FIGURE 2


MICROGRAPHS OF ATTRITED POWDER OF ALLOY A

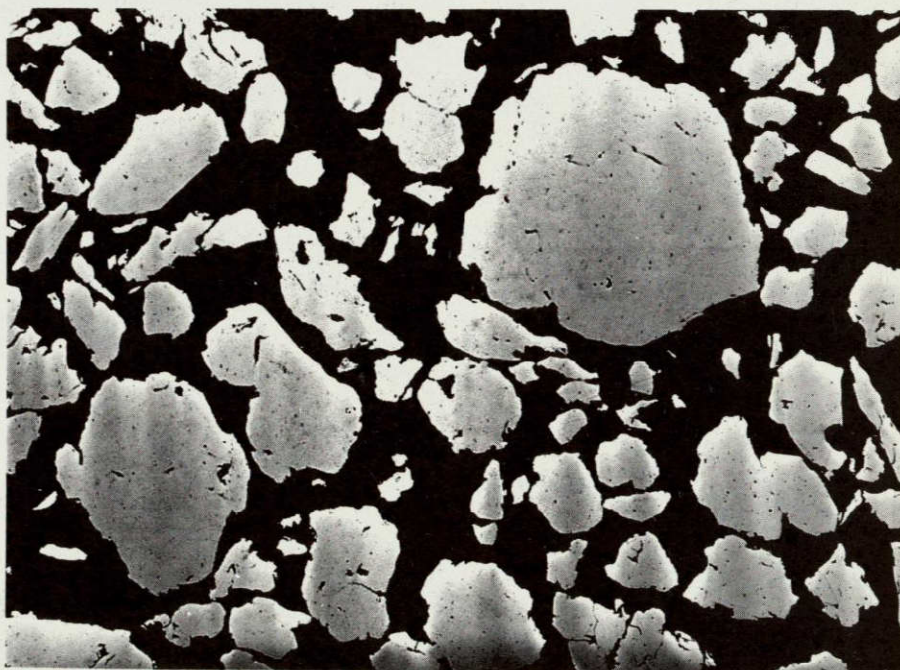




P.N. 1-48507

(a) Alloy B - Powder Batch N3

 40 $\mu$ m



P.N. 1-48509

(b) Alloy C - Powder Batch N4

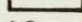
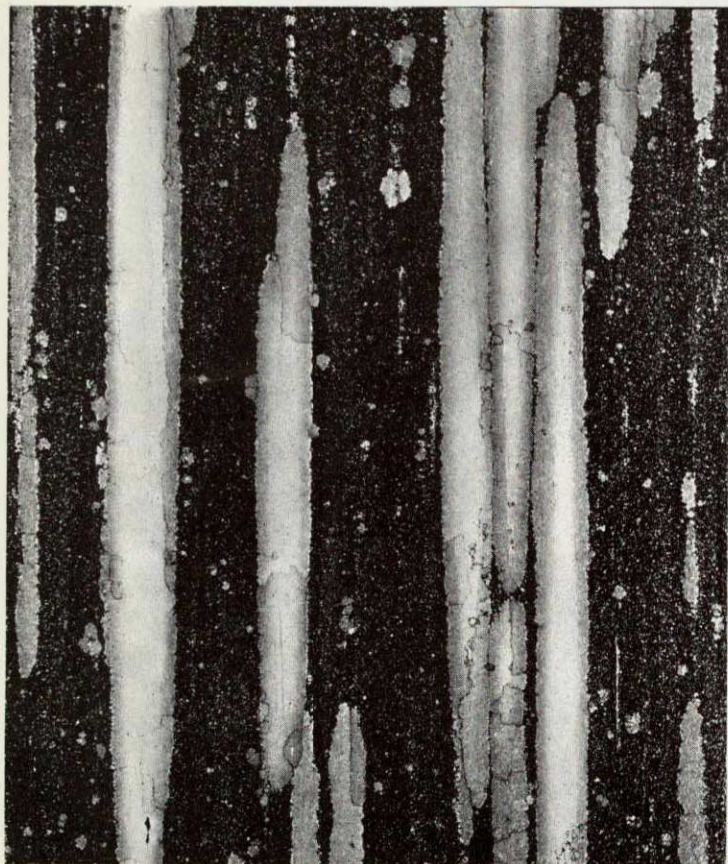
 40 $\mu$ m

FIGURE 3

MICROGRAPHS OF ATTRITED POWDER OF ALLOYS B AND C

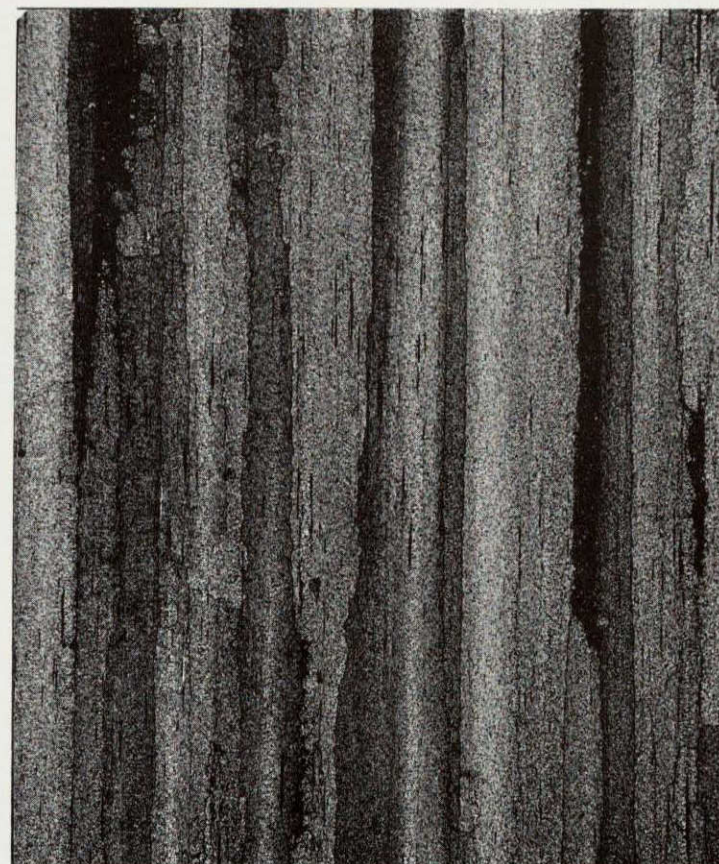




P.N. 1-49541

50X

(a) 12:1, 5.3 cm/sec.



P.N. 1-49539

50X

(b) 22:1, 4.3 cm/sec.

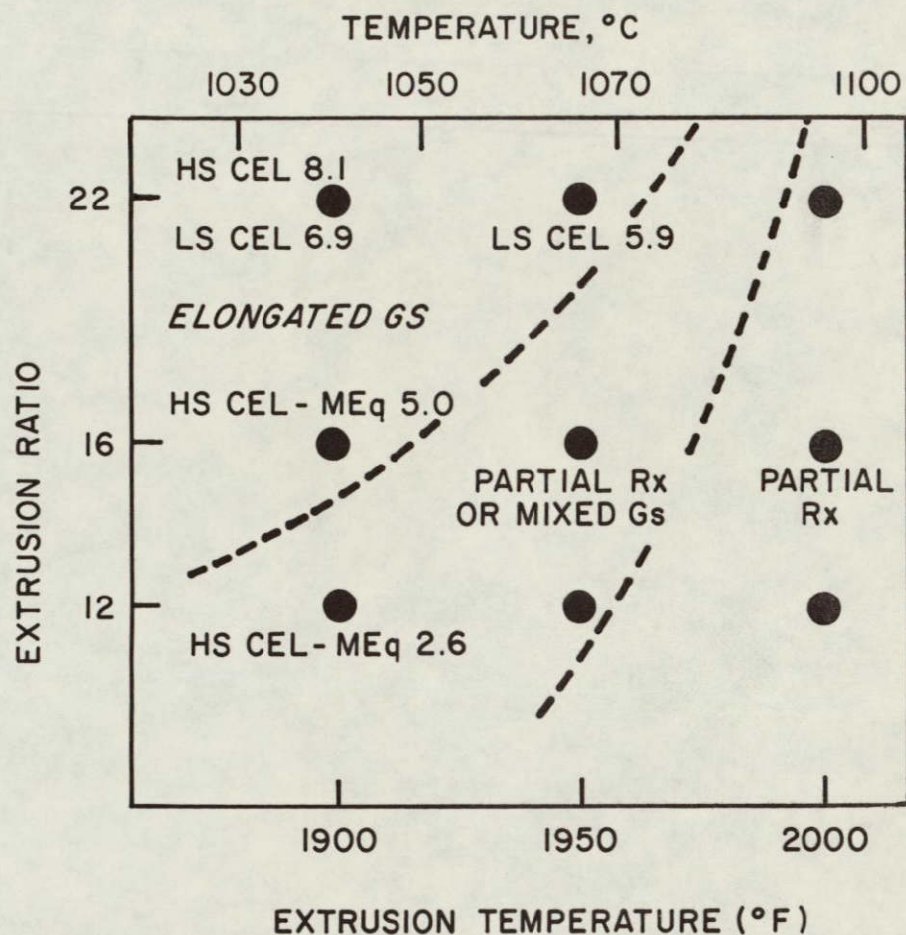
#### FIGURE 4

MICROSTRUCTURES OF 1066°C (1950°F) EXTRUSIONS AND CONVENTIONALLY ANNEALED  
(1232°C/0.5 HR/AC)

(a) Extrusion Ratio 12:1, Ram Speed 5.3 cm/sec.

(b) Extrusion Ratio 22:1, Ram Speed 4.3 cm/sec.



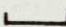


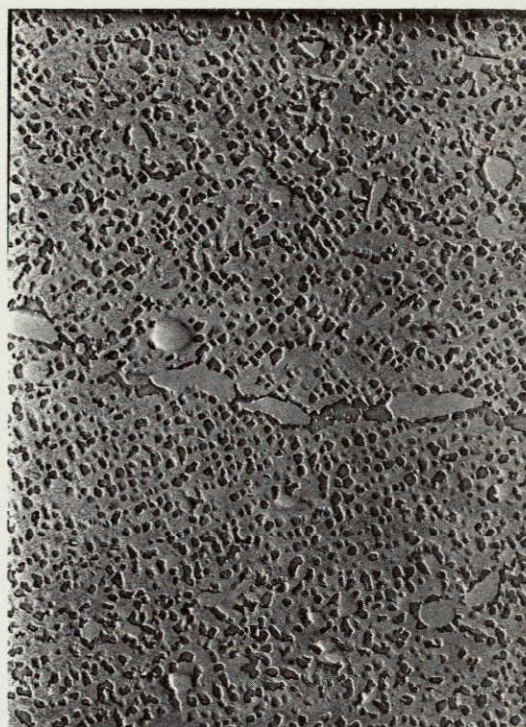
**FIGURE 5 - EXTRUSION RATIO - TEMPERATURE MAP SHOWING ZONES OF RECRYSTALLIZATION RESPONSE. (ALLOY A)**  
 HS = HIGH SPEED EXTRUSION  
 LS = LOW SPEED EXTRUSION  
 GS = GRAIN STRUCTURE  
 CEL = COARSE ELONGATED  
 Rx = RECRYSTALLIZED  
 NUMBERS REFER TO GRAIN LENGTH TO DIAMETERS RATIO (GAR)





EM-18501

  
1.6  $\mu\text{m}$



EM-18502


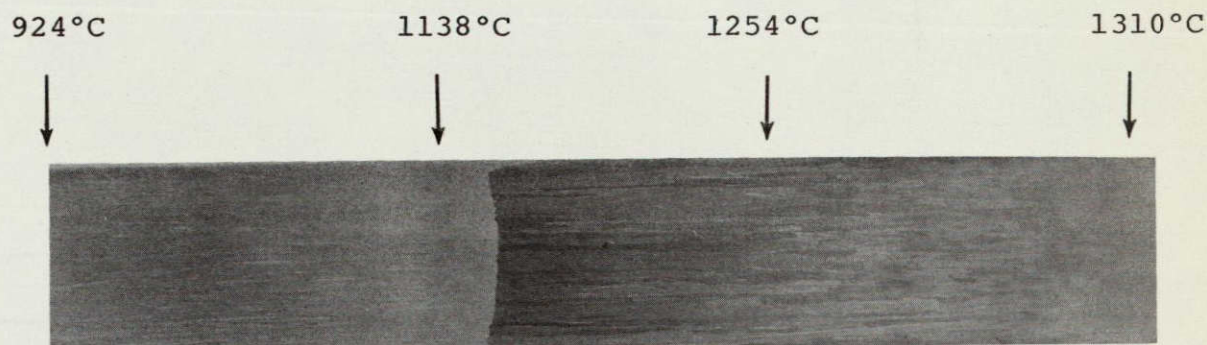
  
1.6  $\mu\text{m}$

FIGURE 6

ELECTRON MICROGRAPHS SHOWING THE STRUCTURE OF  
ALLOY A AFTER EXPOSURE AT 816°C (1500°F)  
AND 207 MPa (30 KSI) FOR 2000 HOURS.  
SAMPLE ANNEALED 0.5 HOUR/1232°C (2250°F)/AC  
PRIOR TO EXPOSURE.

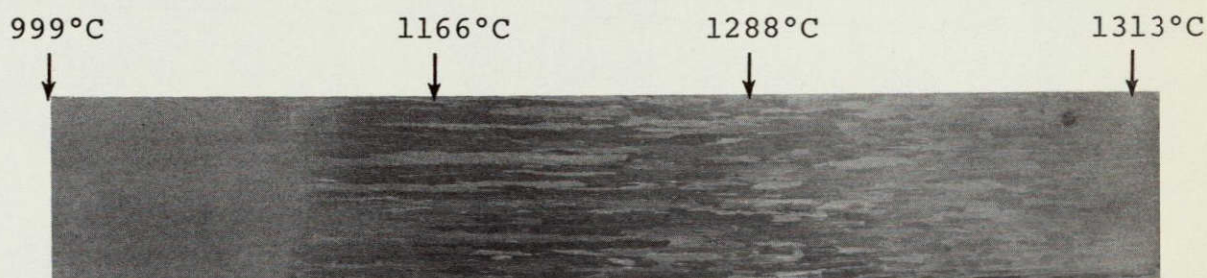




P.N. 2-56107

2X

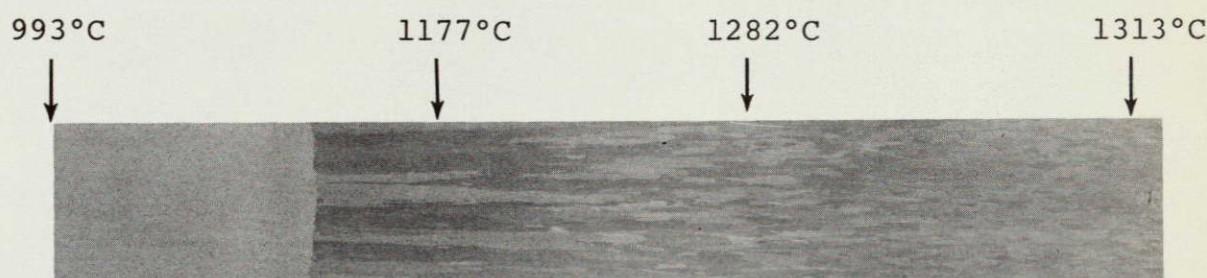
A: Extruded at 1038°C(1900°F), 16:1 Ratio, 7.62 cm/sec Speed



P.N. 2-56107

2X

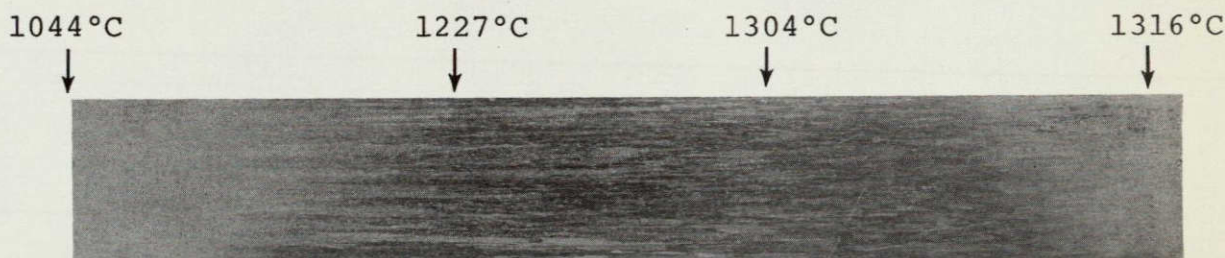
B: Extruded at 1038°C(1900°F), 16:1 Ratio, 20.3 cm/sec Speed



P.N. 2-56108

2X

C: Extruded at 1038°C(1900°F), 20:1 Ratio, 7.62 cm/sec Speed



P.N. 2-56108

2X

D: Extruded at 1038°C(1900°F), 20:1 Ratio, 20.3 cm/sec Speed

FIGURE 7

MACROSTRUCTURES OF GRADIENT ANNEALED N39 EXTRUDED  
BAR (A-D)



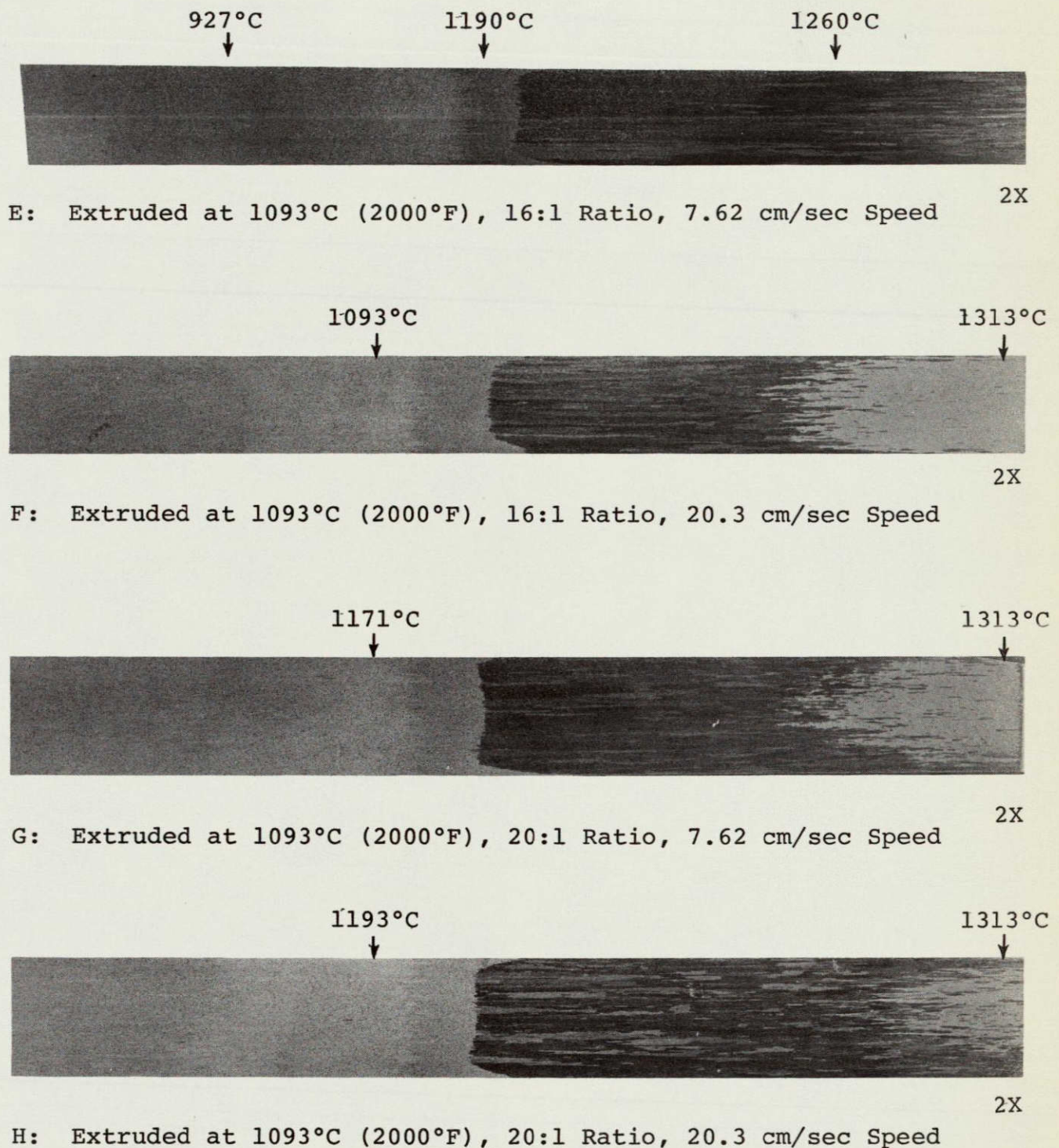
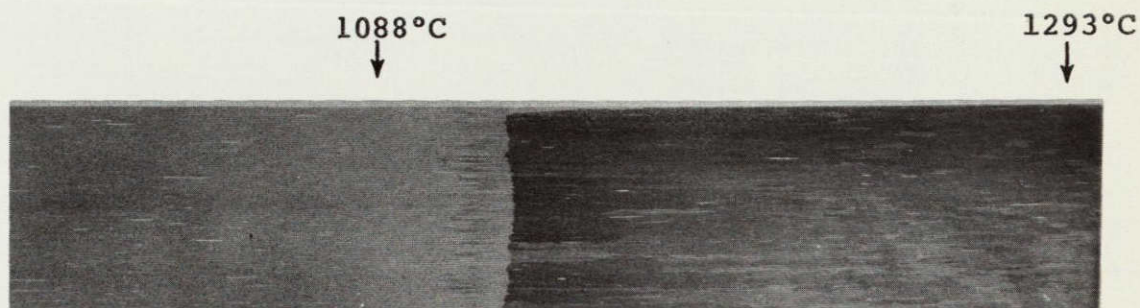


FIGURE 8

MACROSTRUCTURES OF GRADIENT ANNEALED N39 EXTRUDED BAR (E-H)

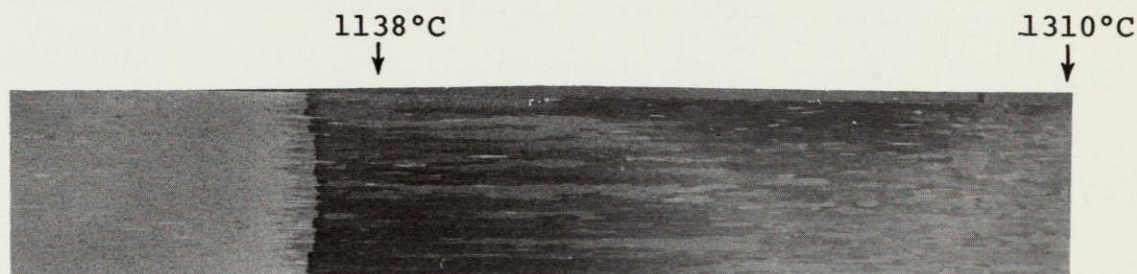




P.N. 2-56112

2X

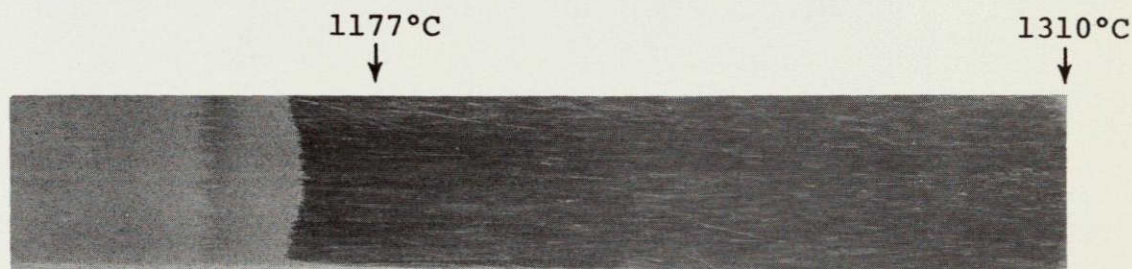
A. N40A: Extruded at 1038°C (1900°F), 16:1 Ratio,  
7.62 cm/sec Speed



P.N. 2-56112

2X

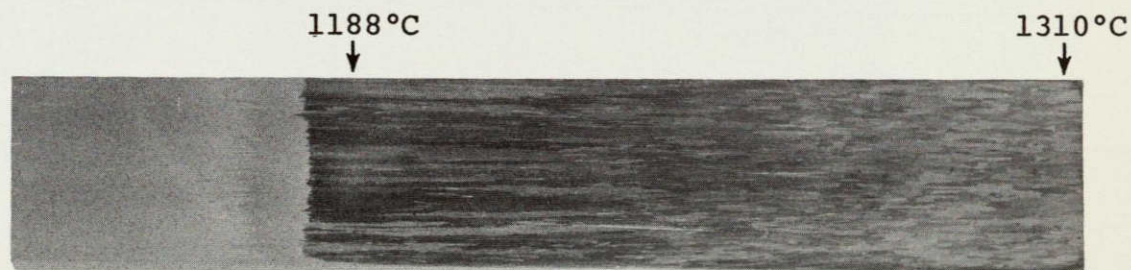
B. N40C: Extruded at 1038°C (1900°F), 20:1 Ratio,  
7.62 cm/sec Speed



P.N. 2-56109

2X

C. N48A: Extruded at 1038°C (1900°F), 16:1 Ratio,  
7.62 cm/sec Speed



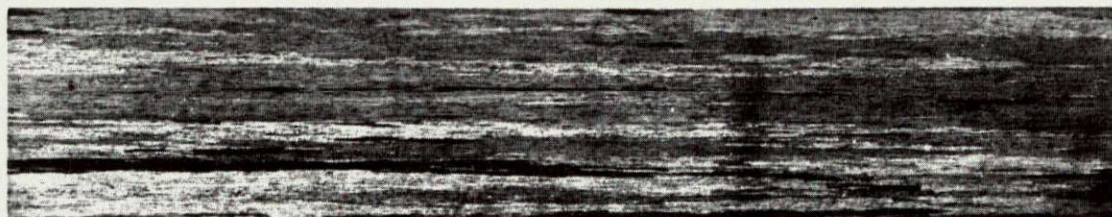
P.N. 2-56110

2X

D. N48C: Extruded at 1038°C (1900°F), 20:1 Ratio,  
7.62 cm/sec Speed

FIGURE 9

MACROSTRUCTURE OF GRADIENT ANNEALED BAR OF  
N40 AND N48



P.N. 2-59987

1.5X

FIGURE 10

MACROSTRUCTURE OF EXTRUDED (16:1 RATIO, 20.3 cm/sec, 1038°C)  
AND ZONE ANNEALED N39B BAR.

NOTE COARSE ELONGATED GRAINS (GAR >10:1)



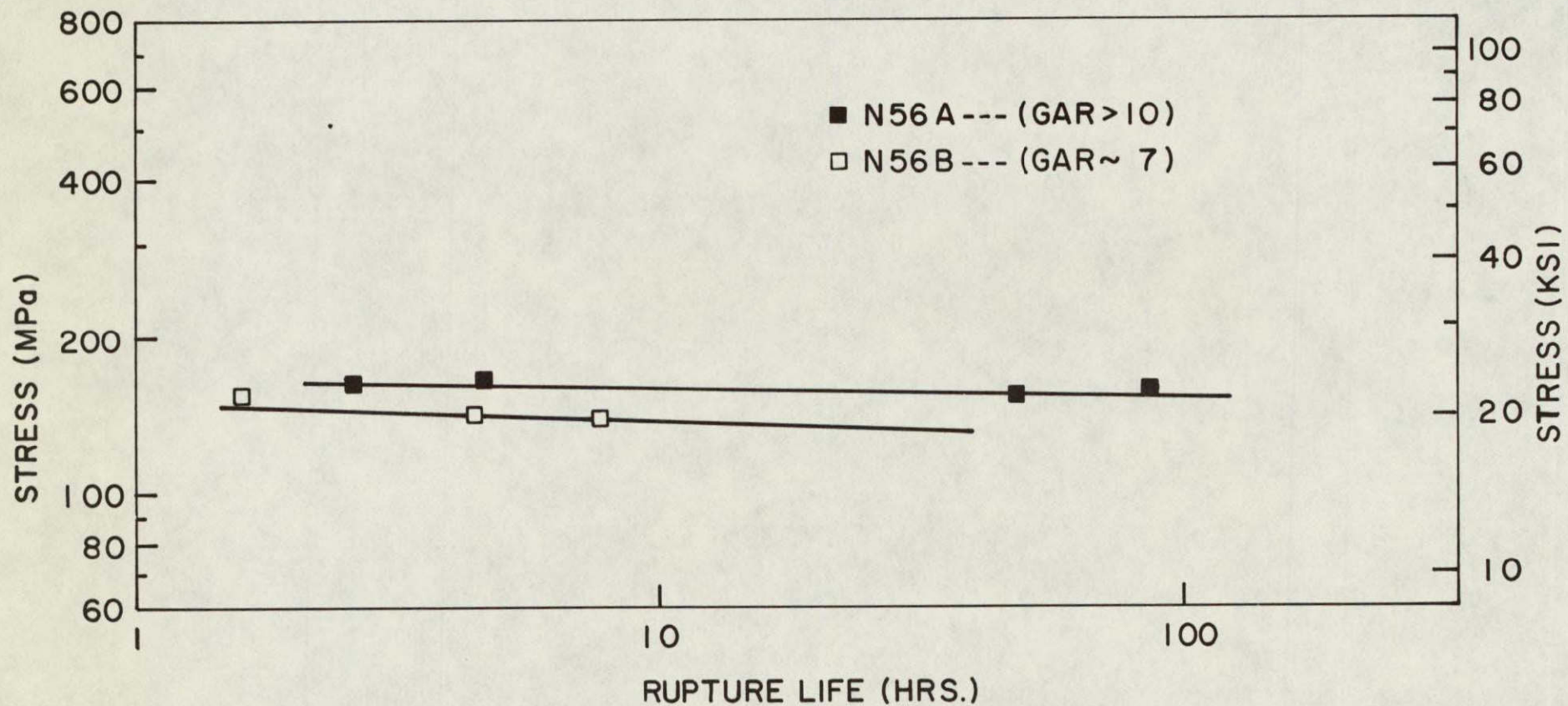
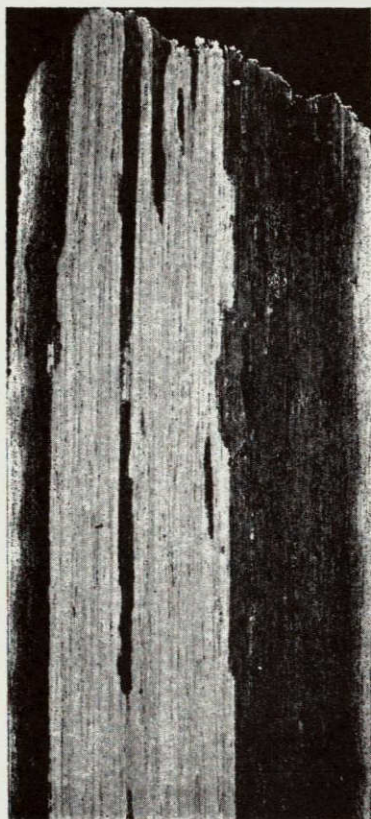


FIGURE II - STRESS-RUPTURE PROPERTIES OF N56A AND N56B BARS AT 1093°C (2000°F).



P.N. 1-56598      20X  
 (a) N56-A4 (GAR 10+)

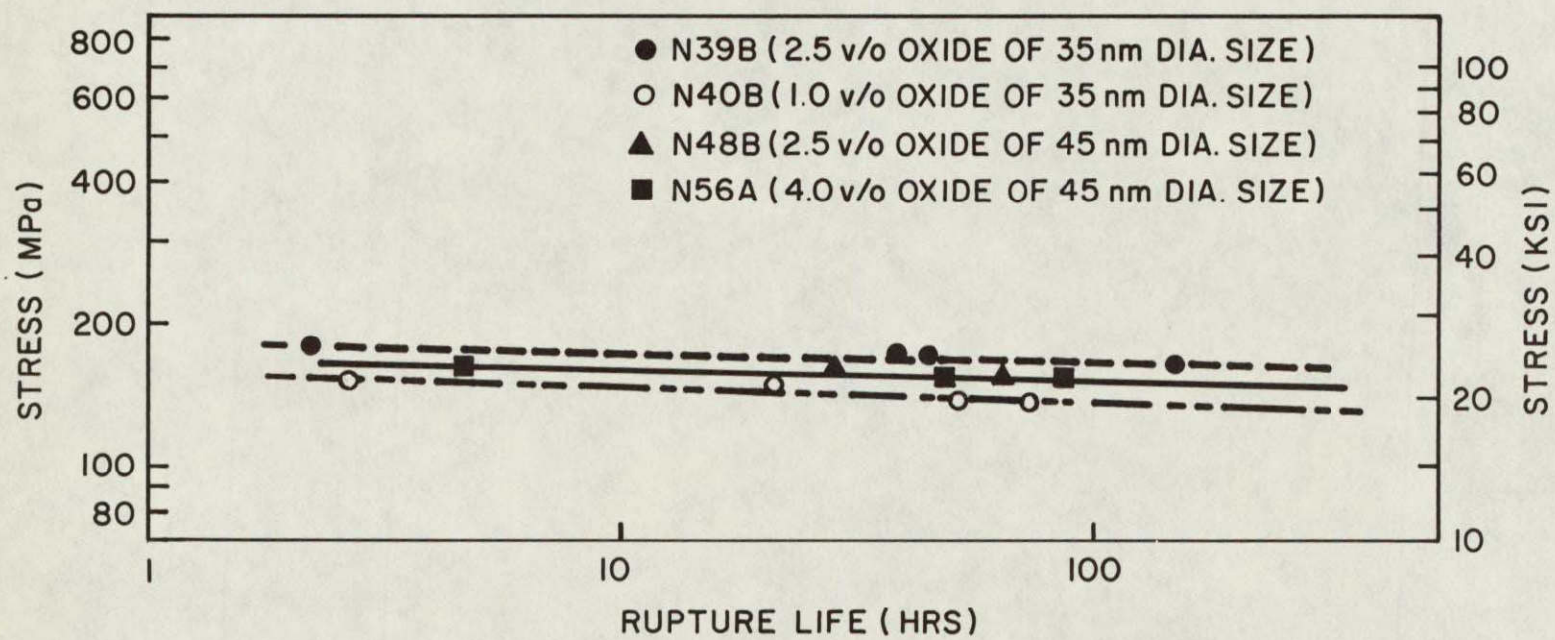


P.N. 1-56599      20X  
 (b) N56-B1 (GAR ~7)

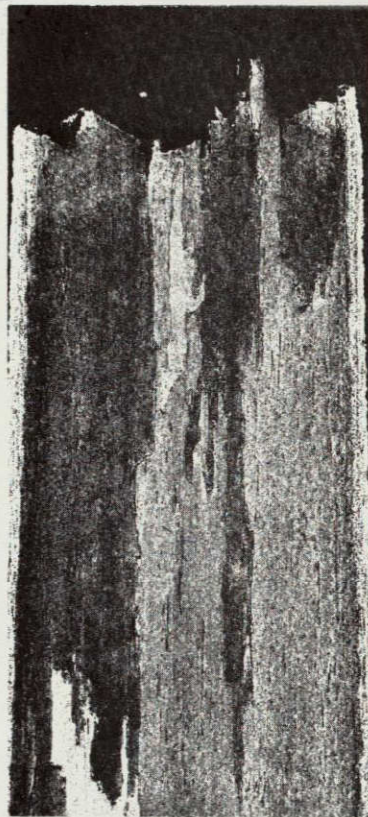
FIGURE 12

LONGITUDINAL SECTIONS OF RUPTURED N56 ALLOYS  
 TESTED AT 1093°C (2000°F)

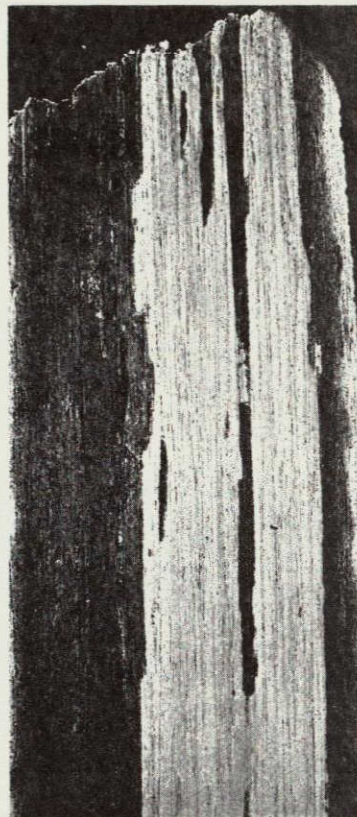




**FIGURE 13** - STRESS - RUPTURE PROPERTIES OF N39B, N40B, N48B AND N56B BARS  
AT 1093°C (2000°F).



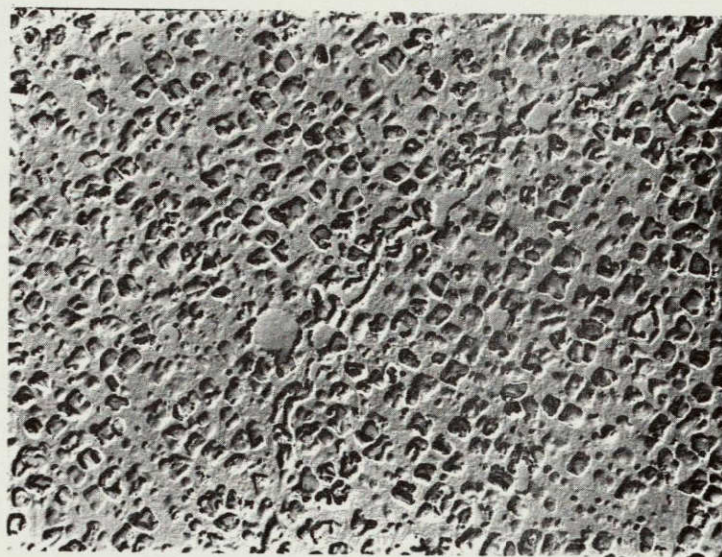
P.N. 1-56596      20X  
(a) N39-B5



P.N. 1-56598      20X  
(b) N56-A4

FIGURE 14  
LONGITUDINAL GRAIN STRUCTURES OF  
N39-B AND N56-A



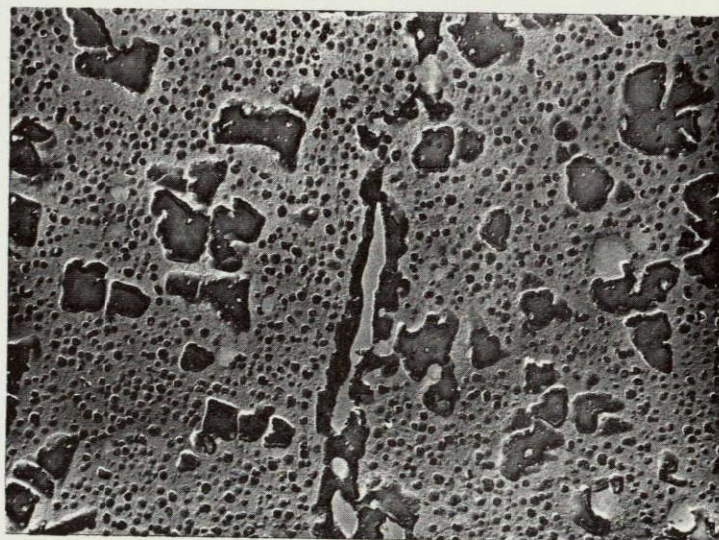


EM-019458

0.87 $\mu$ m

FIGURE 15

MICROSTRUCTURE OF N39B-1H: ZONE ALLEALED  
AT 1232°C (2250°F), 13.5 cm/HR +  
HEAT TREATMENT 1 (1/2 HR/1232°C (2150°F)/  
AC + 24 HRS/843°C (1550°F)/AC)



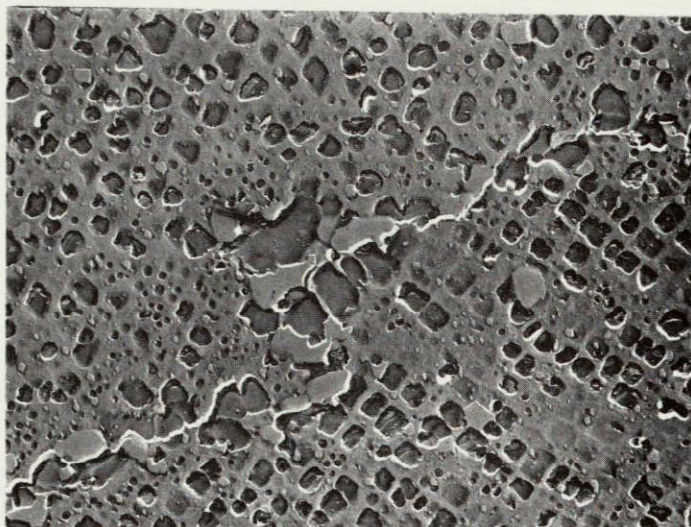
EM-019448

0.87 $\mu$ m

FIGURE 16

MICROSTRUCTURE OF N39B-2H: ZONE ANNEALED  
AT 1232°C (2250°F), 13.5 cm/HR +  
HEAT TREATMENT 2 (1/2 HR/1232°C (2150°F)/  
FURNACE COOLED TO 1066°C (1950°F)/AC +  
24 HRS/843°C (1550°F)/AC)



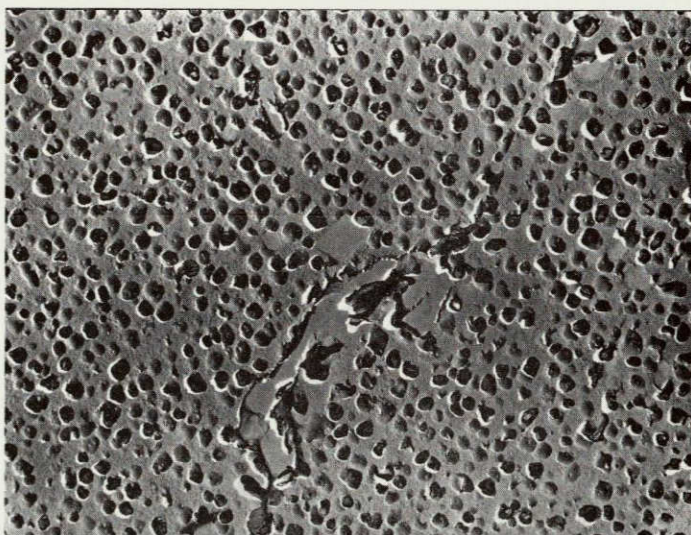


EM-019462

0.87μm

FIGURE 17

MICROSTRUCTURE OF N39B-3H: ZONE ANNEALED  
AT 1232°C (2250°F), 13.5 cm/HR +  
HEAT TREATMENT 3 (1/2 HR/1232°C (2250°F)/  
AC + 2 HRS/1066°C (1910°F)/AC +  
24 HRS/843°C (1550°F)/AC)



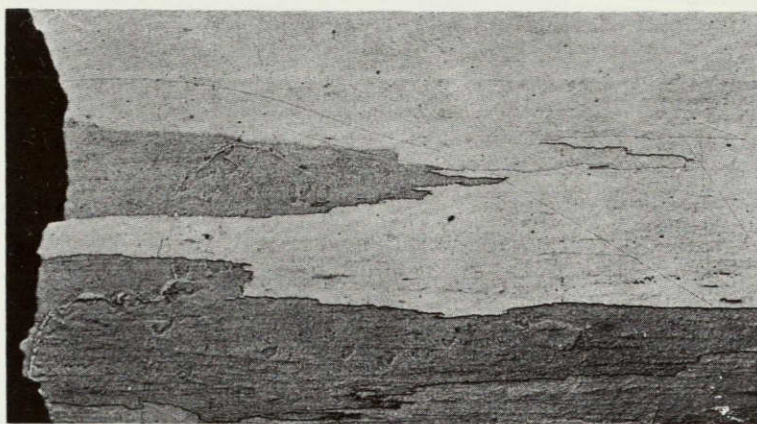
EM-019471

0.87μm

FIGURE 18

MICROSTRUCTURE OF N39B-4H: ZONE ANNEALED  
AT 1232°C (2250°F), 13.5 cm/HR +  
HEAT TREATMENT 4 (1/2 HR/1232°C (2250°F)/  
AC + 2 HRS/954°C (1750°F)/AC +  
24 HRS/843°C (1550°F)/AC)





P.N. 1-57818

20X

(a) N39B-1H-1: Zone Annealed at  
1232°C (2250°F), 13.5 cm/Hr +  
Heat Treatment 1 (1/2 Hr/1232°C  
(2250°F)/AC + 24 Hrs/843°C  
(1550°F)/AC)



P.N. 1-57820

20X

(b) N39B-4H-2: Zone Annealed at  
1232°C (2250°F), 13.5 cm/Hr +  
Heat Treatment 4 (1/2 Hr/1232°C  
(2250°F)/AC + 2 Hrs/954°C  
(1750°F)/AC + 24 Hrs/843°C  
(1550°F)/AC)

# FIGURE 19

FRACTURE PROFILES OF SPECIMENS OF N39B STRESS  
RUPTURE TESTED AT 760°C (1400°F). NOTE  
TRANSGRANULAR FRACTURES.

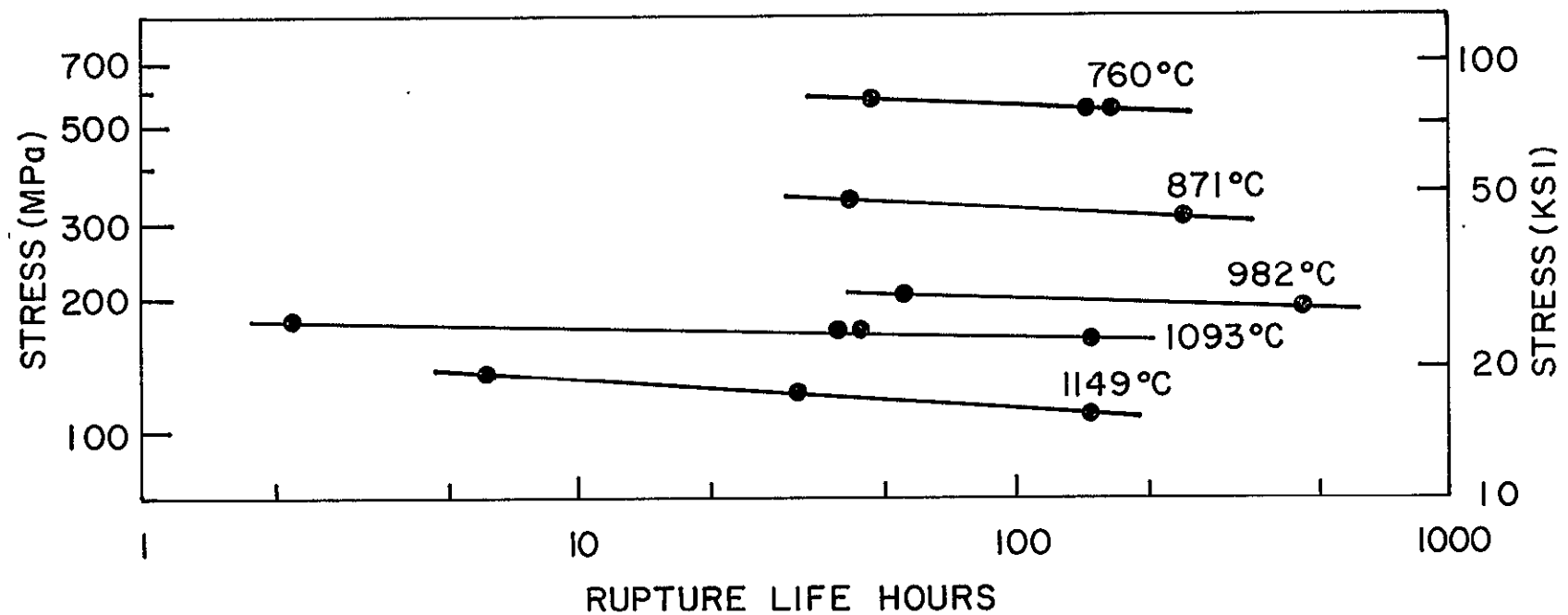


FIGURE 20- SUMMARY PLOT OF RUPTURE PROPERTIES OF ALLOY D.

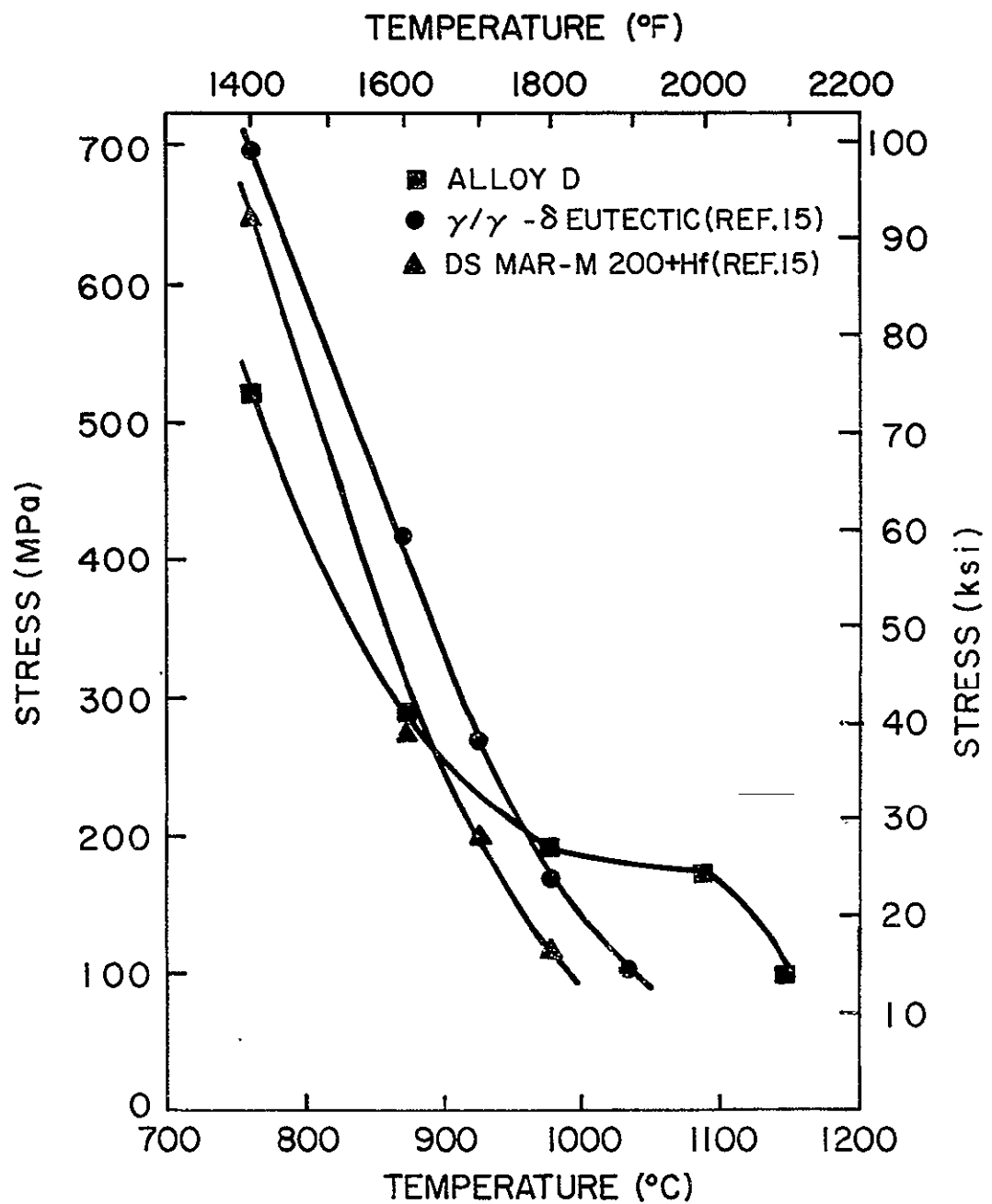
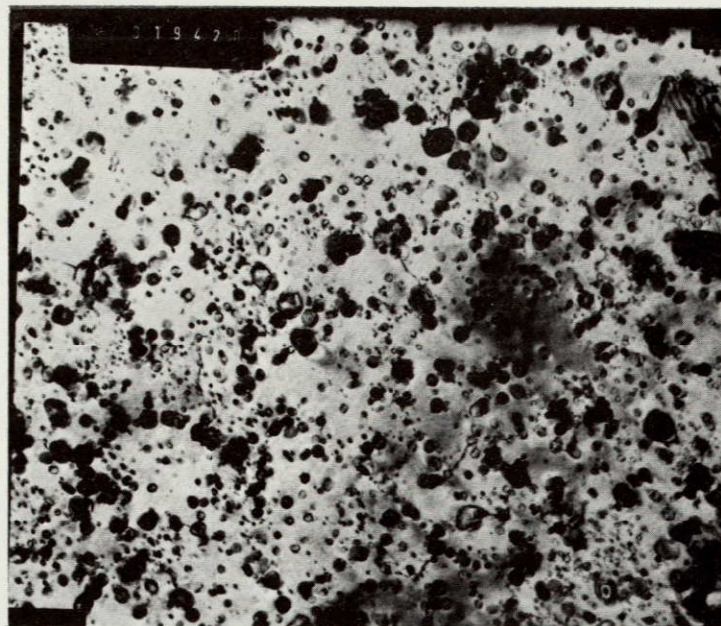


FIGURE 21-COMPARISON OF 1000 HOUR RUPTURE STRENGTH CAPABILITY OF ALLOY D WITH DS MAR-M 200+Hf AND  $\gamma/\gamma' - \delta$  EUTECTIC ALLOY.

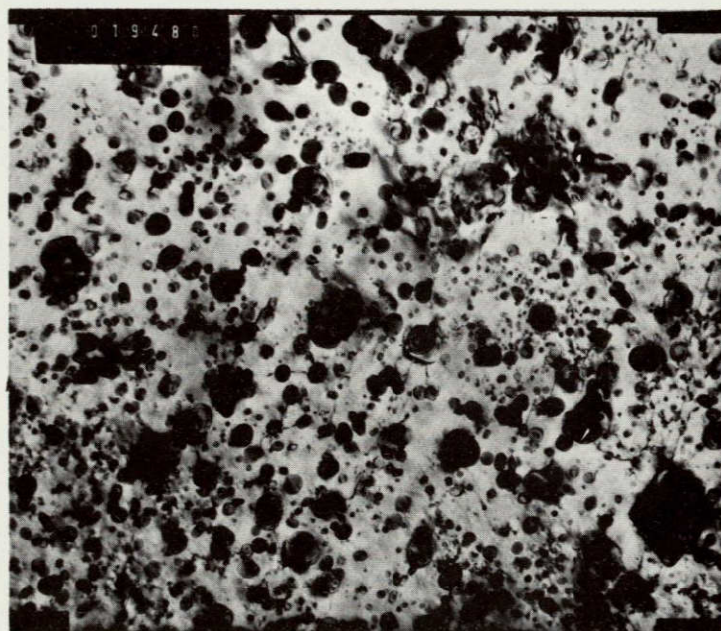




EM-019420

(a) N39A

0.24 $\mu$ m



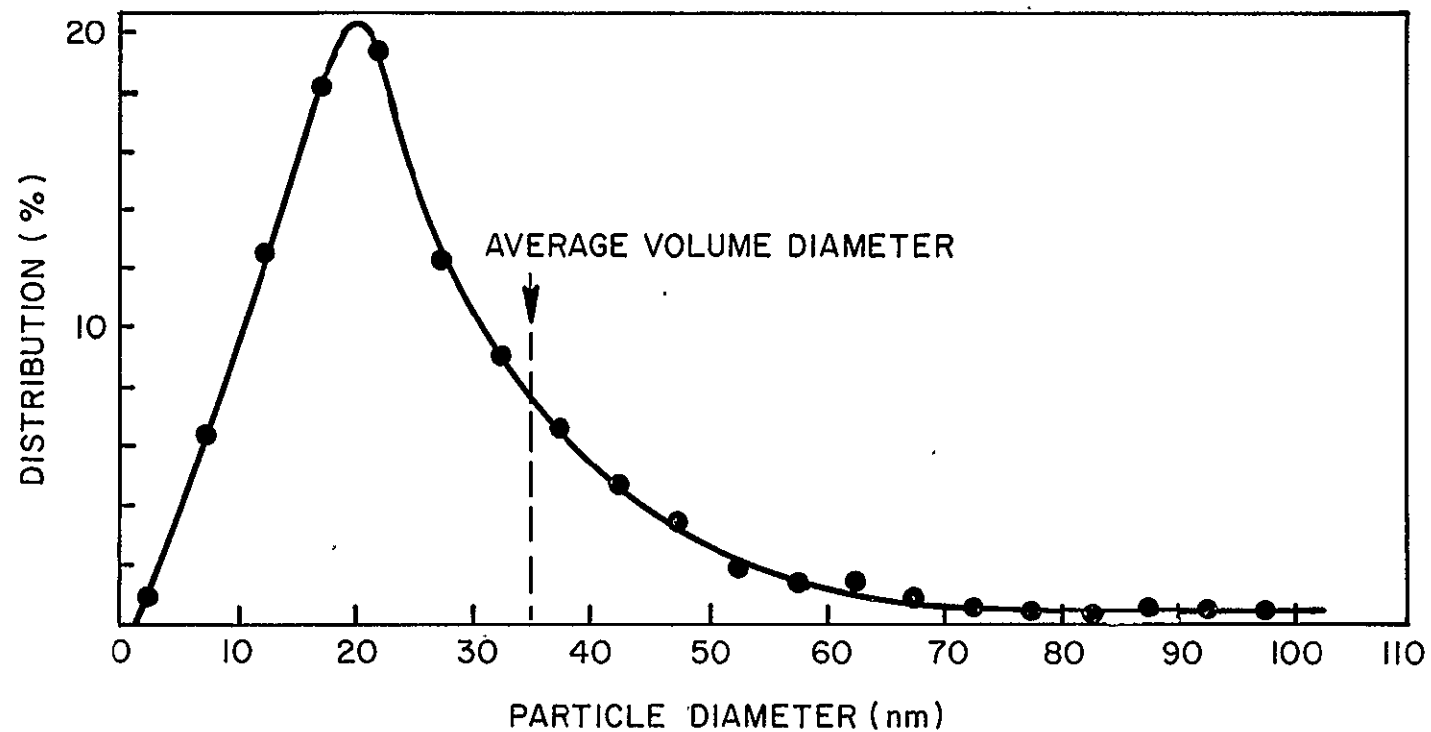
EM-019480

(b) N48A

0.24 $\mu$ m

FIGURE 22

THIN FOIL TRANSMISSION ELECTRON MICROGRAPHS  
SHOWING DISPERSOID PARTICLES IN ZONE  
ANNEALED PLUS HEAT TREATED  
(0.5 HR/1232°C/WQ) N39A AND N48A BARS



**FIGURE 23 - DISPERSOID PARTICLE SIZE DISTRIBUTION FOR ANNEALED N39 BAR  
(704°C (1300°F) CALCINATION TREATMENT)**

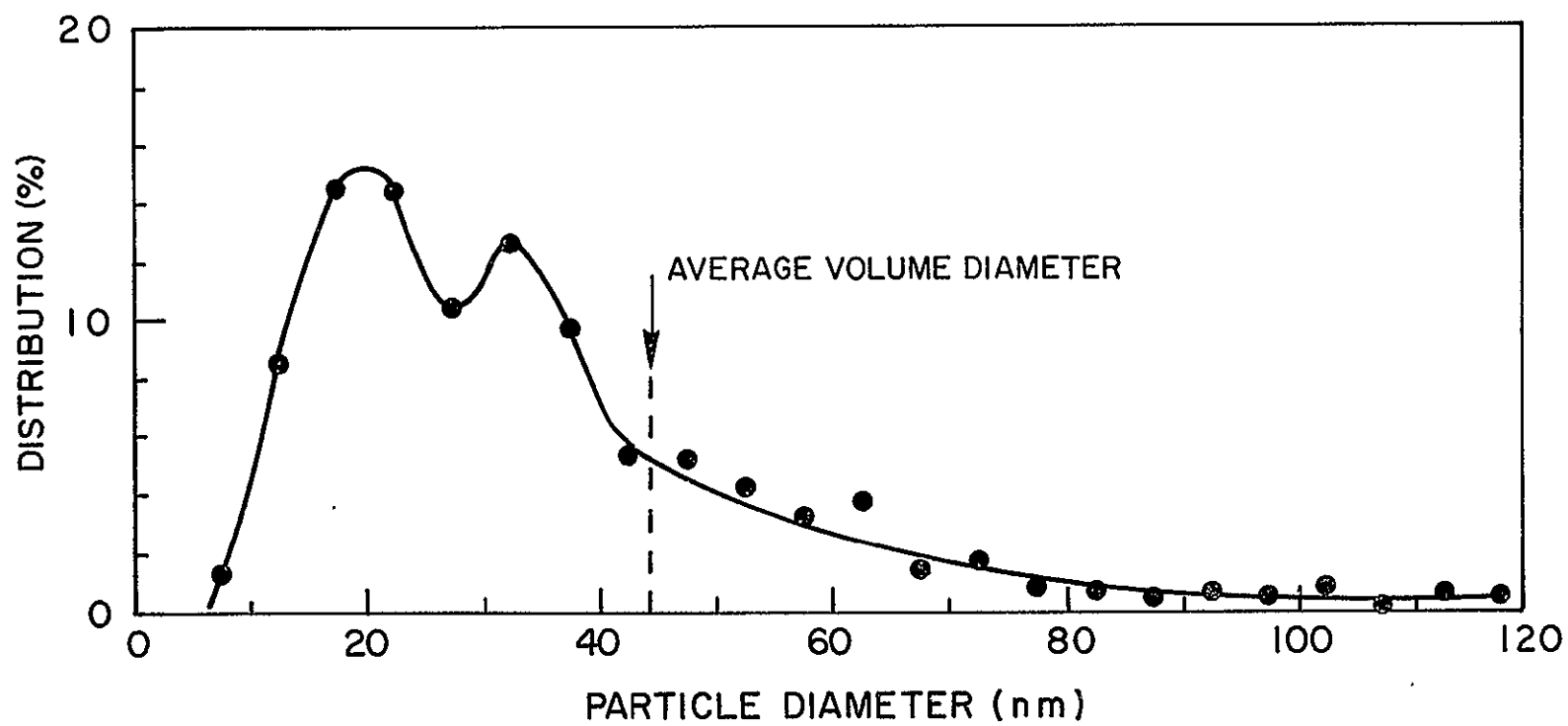


FIGURE 24 - DISPERSOID PARTICLE SIZE DISTRIBUTION FOR ANNEALED N48 BAR (1500°C (2732 °F) CALCINATION TREATMENT).

DISTRIBUTION LIST FOR NASA CR-135150

CONTRACT NAS3-19694

(THE NUMBER IN PARENTHESES SHOWS HOW MANY COPIES  
IF MORE THAN ONE ARE TO BE SENT TO AN ADDRESS.)

MR. J. ACURIO

MS 77-5

NASA LEWIS RESEARCH CTR.  
21000 BROOKPARK ROAD  
CLEVELAND, OHIO 44135

MR. A.E. ANGLIN

MS 49-3

NASA LEWIS RESEARCH CTR.  
21000 BROOKPARK ROAD  
CLEVELAND, OHIO 44135

MR. G.T. ROLL

MS 3-5

NASA LEWIS RESEARCH CTR  
21000 BROOKPARK ROAD  
CLEVELAND, OHIO 44135

MR. C.P. BLANKENSHIP

MS 105-1

NASA LEWIS RESEARCH CTR  
21000 BROOKPARK ROAD  
CLEVELAND, OHIO 44135

MR. T.K. GLASGOW (30)

MS 49-3

NASA LEWIS RESEARCH CTR.  
21000 BROOKPARK ROAD  
CLEVELAND, OHIO 44135

DR. H.R. GRAY

MS 49-3

NASA LEWIS RESEARCH CTR.  
21000 BROOKPARK ROAD  
CLEVELAND, OHIO 44135

MR. F.H. HARF

MS 49-3

NASA LEWIS RESEARCH CTR  
21000 BROOKPARK ROAD  
CLEVELAND, OHIO 44135

MR. C.E. LOWELL

MS 49-3

NASA LEWIS RESEARCH CTR.  
21000 BROOKPARK ROAD  
CLEVELAND, OHIO 44135

M & S DIVISION FILES

MS 49-1

NASA LEWIS RESEARCH CTR  
21000 BROOKPARK ROAD  
CLEVELAND, OHIO 44135

DR. H.B. PROBST

MS 49-3

NASA LEWIS RESEARCH CTR.  
21000 BROOKPARK ROAD  
CLEVELAND, OHIO 44135

MR. N.T. SAUNDERS

MS 105-1

NASA LEWIS RESEARCH CTR  
21000 BROOKPARK ROAD  
CLEVELAND, OHIO 44135

MR. R.A. SIGNORELLI

MS 106-1

NASA LEWIS RESEARCH CTR.  
21000 BROOKPARK ROAD  
CLEVELAND, OHIO 44135

MR. J.W. WEETON

MS 106-1

NASA LEWIS RESEARCH CTR.  
21000 BROOKPARK ROAD  
CLEVELAND, OHIO 44135

DR. J.D. WHITTENBERGER

MS 105-1

NASA LEWIS RESEARCH CTR.  
21000 BROOKPARK ROAD  
CLEVELAND, OHIO 44135

DR. W.F. SCHILLING  
MATERIALS & PROCESSES LAB  
GENERAL ELECTRIC COMPANY  
SCHENECTADY, NY 12345

LIBRARY  
ADVANCED TECHNOLOGY LAB  
GENERAL ELECTRIC COMPANY  
SCHENECTADY, NY 12345

MR. C.T. SIMS  
GAS TURBINE PROD.DIV.  
GENERAL ELECTRIC COMPANY  
SCHENECTADY, N.Y. 12345

MR. G.E. WASIELEWSKI  
MATERIALS & PROCESSES LAB  
GENERAL ELECTRIC COMPANY  
SCHENECTADY, N.Y. 12345

TECHN. INFORMATION CENTER  
AEG  
GENERAL ELECTRIC COMPANY  
CINCINNATI, OHIO 45215

MR. P.G. BAILEY  
AEG/GED  
GENERAL ELECTRIC COMPANY  
CINCINNATI, OHIO 45215

DR. M. HERMAN  
DETROIT DIESEL ALLISON DV  
P.O. BOX 894  
INDIANAPOLIS, IN 46206

MR. E.S. NICHOLS PT.8 T2B  
DETROIT DIESEL ALLISON DV  
P.O. BOX 894  
INDIANAPOLIS, IN 46206

MR. G.S. MANN  
GENERAL MOTORS CORP.  
AC SPARK PLUG DIV  
1300 N. DIXIE HIGHWAY  
FLINT, MI 48556

MR. R.J. NYLEN  
HOMOGENOUS METALS INC.  
WEST CANADA BLVD  
HERKIMER, N.Y. 13350

MR. A. STETSON  
SOLAR DIVISION  
INTERNATIONAL HARVESTER  
2200 PACIFIC HIGHWAY  
SAN DIEGO, CAL. 92112

DR. J. BENJAMIN  
INTERNATIONAL NICKEL CO.  
MERICA RESEARCH LAB  
STERLING FOREST  
SUFFERN, NY 10901

MR. J. DEBORD  
HUNTINGTON ALLOYS DIV.  
INTERNATIONAL NICKEL CO.  
HUNTINGTON, WV 25720

MR. J.P. MORSE  
HUNTINGTON ALLOYS DIV.  
INTERNATIONAL NICKEL CO.  
HUNTINGTON, WV 25720

MR. D.J. TILLACK  
HUNTINGTON ALLOYS DIV.  
INTERNATIONAL NICKEL CO.  
HUNTINGTON, WV 25720

MR. T. MILES  
KELSEY HAYES CORPORATION  
7250 WHITMORE LAKE ROAD  
BRIGHTON, MI 48116



TECHNICAL INFORMATION CTR.  
MATLS. & SCIENCE LAB.  
LOCKHEED RESEARCH LABS  
3251 HANOVER STREET  
PALO ALTO, CAL. 94304

MR. W. PRECHT  
MARTIN-MARIETTA LABS.  
1450 SOUTH ROLLING ROAD  
BALTIMORE, MD 21227

LIBRARY MSFD  
MCDONNELL DOUGLAS CORP.  
3000 OCEAN PARK BLVD  
SANTA MONICA, CAL. 90406

MR. G.I. FRIEDMAN  
NUCLEAR METALS, INC.  
229 MAIN STREET  
CONCORD, MA 01742

ROCKWELL INTERNATIONAL  
ROCKETDYNE DIVISION  
6633 CANOGA AVENUE  
CANOGA PARK, CA 91304

DR. S. BARANOW  
SPECIAL METALS  
CORPORATION  
NEW HARTFORD, N.Y. 13413

MR. F. ELLIOT  
TELEDYNE-ALLVAC  
P.O. BOX 759  
MONROE, NC 28110

DR. R. BECK  
TELEDYNE-CAE  
1330 LASKEY ROAD  
TOLEDO, OH 43601

MR. A.R. KAUFMAN  
TEXTRON INC.  
WEST CONCORD, MA  
01781

DR. C.S. KORTOVICH  
MATERIALS TECHNOLOGY  
TRW EQUIPMENT GROUP  
23555 EUCLID AVENUE  
CLEVELAND, OHIO 44117

MR. D. MORACZ  
MATERIALS TECHNOLOGY  
TRW EQUIPMENT GROUP  
23555 EUCLID AVENUE  
CLEVELAND, OHIO 44117

MR. L. ENGEL  
TURBODYNE CORPORATION  
711 ANDERSON AVE., N.  
ST. CLOUD, MN 56301

DR. E.R. THOMPSON  
UNITED TECHNOLOGIES CORP  
RESEARCH CENTER  
EAST HARTFORD, CT  
06108

RESEARCH LIBRARY  
UNITED TECHNOLOGIES CORP  
400 MAIN STREET  
EAST HARTFORD, CT  
06108

DR. R.H. BARKALOW  
PRATT & WHITNEY AIRCRAFT  
UNITED TECHNOLOGIES CORP  
400 MAIN STREET  
EAST HARTFORD, CT 06108

DR. M.L. GELL  
PRATT & WHITNEY AIRCRAFT  
UNITED TECHNOLOGIES CORP  
400 MAIN STREET  
EAST HARTFORD, CT 06108

CONTRACTS SECTION B  
MS 500-313  
NASA LEWIS RESEARCH CTR  
21000 BROOKPARK ROAD  
CLEVELAND, OH 44135

REPORT CONTROL OFFICE  
MS 5-5  
NASA LEWIS RESEARCH CTR  
21000 BROOKPARK ROAD  
CLEVELAND, OHIO 44135

MAJ. F.J. GASPERICH  
AFSC LIAISON MS 501-3  
NASA LEWIS RESEARCH CTR  
21000 BROOKPARK ROAD  
CLEVELAND, OHIO 44135

MR. J. GANGLER / RWM  
NASA HEADQUARTERS  
WASHINGTON, DC  
20546.

MR. B.A. STEIN  
NASA  
LANGLEY RESEARCH CENTER  
HAMPTON, VA 23365

MR. E.A. HASEMEYER  
NASA  
MARSHALL SPACE FLIGHT  
CENTER  
AL 35812

TECHNICAL LIBRARY / JM6  
NASA  
JOHNSON SPACE CENTER  
HOUSTON, TX 77058

LIBRARY  
NASA  
DRYDEN FLIGHT RES. CTR  
P. O. BOX 272  
EDWARDS, CA 93523

LIBRARY (2)  
MS 60-3  
NASA LEWIS RESEARCH CTR  
21000 BROOKPARK ROAD  
CLEVELAND, OHIO 44135

TECHNOLOGY UTILIZATION  
MS 3-19  
NASA LEWIS RESEARCH CTR  
21000 BROOKPARK ROAD  
CLEVELAND, OHIO 44135

MR G. C. DEUTSCH / RW  
NASA HEADQUARTERS  
WASHINGTON, DC  
20546

LIBRARY  
NASA  
GODDARD SPACE FLIGHT CTR  
GREENBELT, MARYLAND 20771

LIBRARY  
NASA  
LANGLEY RESEARCH CENTER  
HAMPTON, VA 23365

LIBRARY  
NASA  
MARSHALL SPACE FLIGHT  
CENTER  
AL 35812

LIBRARY - ACQUISITIONS  
JET PROPULSION LAB.  
4800 OAK GROVE DRIVE  
PASADENA, CA 91102

LIBRARY - REPORTS  
MS 202-3  
NASA AMES RESEARCH CENTER  
MOFFETT FIELD, CA 94035

ACCESSIONING DEPT (10)  
NASA SCIENTIFIC & TECHN.  
INFORMATION FACILITY  
BOX 8757  
BALTIMORE, MD 21240

DEFENCE DOCUMENTATION CTR  
CAMERON STATION  
5010 DUKE STREET  
ALEXANDRIA, VIRGINIA  
22314

MR. L. CLARK  
AFML/LTM

MR. J.K. ELBAUM  
AFML/LTM

WRIGHT PATTERSON AFB,  
OH 45433

WRIGHT PATTERSON AFB,  
OH 45433

MR. N. GEYER  
AFML/LLM

MR T. NORBUT  
AFAPL/TBP

WRIGHT PATTERSON AFB,  
OH 45433

WRIGHT PATTERSON AFB,  
OH 45433

MR. L.J. OBERY  
AFAPL/TBD

MR. W. O'HARA  
AFML/LLM

WRIGHT PATTERSON AFB,  
OH 45433

WRIGHT PATTERSON AFB  
OH 45433

LIBRARY  
ARMY MATERIALS AND  
MECHANICS RESEARCH CTR.  
WATERTOWN, MA 02172

MR. I. MACHLIN AIR-52031B  
NAVAL AIR SYSTEMS COMMAND  
NAVY DEPARTMENT  
WASHINGTON, DC 20361

TECHNICAL REPORTS LIBRARY  
ERDA  
WASHINGTON, DC  
20545

MR. M.I. COPELAND  
DEPT. OF INTERIOR  
BUREAU OF MINES  
P.O. BOX 70  
ALBANY, OR 97321

MR. W.C. MCBEE  
DEPT. OF INTERIOR  
BUREAU OF MINES  
P.O. BOX 70  
ALBANY, OR 97321

DR. B.A. WILCOX  
NATIONAL SCIENCE  
FOUNDATION  
WASHINGTON, DC 20550

DR. A.H. CLAUSER  
BATTELLE MEMORIAL INST.  
505 KING AVENUE  
COLUMBUS, OHIO 43201

MCIC  
BATTELLE MEMORIAL INST.  
505 KING AVENUE  
COLUMBUS, OHIO 43201

PROF. L.J. EBERT  
DEPT. OF MET. & MAT. SCI.  
CASE - WESTERN RESERVE U.  
CLEVELAND, OH 44106

DR. J.K. TIEN  
HENRY KRUMB SCH. OF MINES  
COLUMBIA UNIVERSITY  
NEW YORK, NY 10027

PROF. N.J. GRANT  
DEPT. OF METALLURGY  
MASS. INST. OF TECHNOLOGY  
CAMBRIDGE, MA 02139

DR. W.D. NIX  
DEPT. OF MATERIALS SCI.  
STANFORD UNIVERSITY  
PALO ALTO, CALIF. 94305

PROF. O. SHERBY  
DEPT. OF MATERIALS SCI.  
STANFORD UNIVERSITY  
PALO ALTO, CALIF. 94305

DR. W.F. O'BRIEN, JR.  
DEPT. OF MECH. ENG  
VA. POLYTECH INST.  
BLACKSBURG, VA 24061

MR. R.N. WEIDNER  
AEROCAST INDUSTRIES  
7300 NW 43 STREET  
MIAMI, FL 33166

MR. L.J. FIEDLER  
AVCO LYCOMING DIV.  
550 S. MAIN STREET  
STRATFORD, CT 06497

DR. D. WEBSTER  
BOEING COMPANY  
M.A.S.D.  
SEATTLE, WA 98124

DR. R. GRIERSON  
STELLITE DIVISION  
CABOT CORPORATION  
1020 W. PARK AVENUE  
KOKOMO, IN 46901

DR. S.T. WLODEK  
STELLITE DIVISION  
CABOT CORPORATION  
1020 W. PARK AVE  
KOKOMO, IN 46901

LIBRARY  
CABOT CORPORATION  
STELLITE DIVISION  
P.O. BOX 746  
KOKOMO, INDIANA 46901

DR. D.R. MUZYKA  
CARPENTER TECHNOLOGY CORP  
RES. & DEV. CENTER  
P.O. BOX 662  
READING, PA 19603

DR. D.L. SPONSELLER  
CLIMAX MOLYBDENUM COMPANY  
1600 HURON PARKWAY  
ANN ARBOR, MICHIGAN 48106

DR. R.F. KIRBY  
CHIEF, MATERIALS ENG.  
GARRETT AIRESEARCH  
402 S. 36TH STREET  
PHOENIX, AR 85034

MR. R.T. TORGERSON  
CONVAIR AEROSPACE DIV.  
GENERAL DYNAMICS CORP.  
P.O. BOX 1128  
SAN DIEGO, CA 92112

MR. H.A. HAUSER  
PRATT & WHITNEY AIRCRAFT  
UNITED TECHNOLOGIES CORP  
400 MAIN STREET  
EAST HARTFORD, CT 06108

DR. R. BEGLEY  
WESTINGHOUSE RESEARCH LAB  
BEULAH ROAD  
PITTSBURGH, PA 15235

MR. M. QUATINETZ  
CONSULTANT  
30225 WOLF ROAD  
BAY VILLAGE, OH  
44140

DR. W. WALLACE  
NATIONAL AERONAUTICAL EST  
NATIONAL RESEARCH COUNCIL  
MONTREAL ROAD  
OTTAWA ONT CANADA K1A 0R6

MR. R.W. FRASER  
SHERRITT-GORDON MINES  
FORT SASKATCHEWAN  
ALBERTA  
CANADA

DR. L.F. NORRIS  
SHERRITT-GORDON MINES  
FORT SASKATCHEWAN  
ALBERTA  
CANADA

MR. D.H. TIMBRES  
SHERRITT-GORDON MINES  
FORT SASKATCHEWAN  
ALBERTA  
CANADA

DR. M.J. DONACHIE  
MATERIALS ENGINEERING & RES. LAB.  
MAIL STOP EB [F]  
PRATT & WHITNEY AIRCRAFT  
EAST HARTFORD, CT 06108

MR. D.E. PEAERSON  
ROCKWELL INT.  
ROCKETDYNE DIV.  
6633 CANOGA AVE.  
CANOGA PARK CA 91304

DR. G.S. ANSELL, DEAN  
COLLEGE OF ENGINEERING  
RENSSELAER POLYTECHNIC INST.  
TROY, NY 12181